FINAL DEGREE PROJECT

IN

BIOMEDICAL ENGINEERING

# A NOVEL SMART JACKET FOR BLOOD PRESSURE MEASUREMENT BASED ON SHAPE MEMORY ALLOYS

## Technical Report and Annexes


**Author:** David Monràs Álvarez
**Director:** Xavier Rosell
**Co-Director**: Gil Serrancolí

**Session:** June 2019

# Resum

Els teixits intel·ligents amb aplicacions mèdiques ofereixen la possibilitat d'un control continu i no invasiu fet que se'n beneficien pacients i doctors. Per mesurar la pressió sanguínia en prematurs es requereix d'un actuador en miniatura que permeti ésser integrat en el teixit. Per aquest motiu, s'ha dissenyat un actuador basat en els aliatges de memòria de forma que comprimeix com un braçalet d'aire convencional però amb un consum de 3.5W i permet ser controlat per diferent polsos modulables, oferint així diferents nivells de compressió. A més a més, s'ha dissenyat el primer prototip concepte de la jaqueta intel·ligent, fet d'un teixit de fibres naturals que incorpora: un sensor òptic, un sensor de pressió capacitiu amb gran exactitud, el braçalet de força i una taula de control Lilypad Simblee teixible; és rentable, i té un mòdul Bluetooh de Baixa Energia (BBE) per connectar-se a altres dispositius. Tot això, permet que amb la jaqueta intel·ligent es pugui mesurar per primera vegada la pressió sistòlica, diastòlica i ritme cardíac en prematurs utilitzant un mètode semi-oclusiu. Tanmateix, s'ha dissenyat una aplicació mòbil que s'enllaça amb la jaqueta intel·ligent i que permet als doctors fer un seguiment del pacient en tot moment, i realitzar-ne un control remot, mesura de dades i enregistrament d'una forma còmode i intuïtiva que encaixa amb la necessitat d'una millor gestió clínica pel nombre creixent de pacients i és font d'estalvi per als serveis clínics.

# Resumen

Los tejidos inteligentes con aplicaciones médicas ofrecen la posibilidad de un monitoreo continuo y no invasivo; beneficioso para pacientes y doctores. Para medir la presión sanguínea en prematuros se requiere de un actuador en miniatura que permita ser integrado en el tejido. Por este motivo, se ha diseñado un actuador basado en las aleaciones de memoria de forma que comprime como un brazalete de aire convencional pero con un consumo de 3.5W y permite ser controlado con diferentes pulsos modulables, ofreciendo así diferentes niveles de compresión. Además, se ha diseñado el primer prototipo concepto de la chaqueta inteligente hecho de un tejido de fibras naturales que incorpora: un sensor óptico, un sensor de presión capacitivo con gran exactitud, el brazalete de fuerza y una tabla de control Lilypad Simblee tejible; es rentable, y tiene un módulo Bluetooh de Baja Energía (BBE) para conectarse a otros dispositivos. Todo esto, permite que con la chaqueta inteligente se puedan medir por primera vez en el mundo la presión sistólica, diastólica y ritmo cardíaco en prematuros utilizando un método semi-oclusivo. Además, se ha diseñado una aplicación móvil que se enlaza con la chaqueta inteligente y que permite a los doctores hacer un seguimiento del paciente en todo momento, y realizar un control remoto, medición de datos y grabación de una forma cómoda e intuitiva; que encaja con la necesidad de una mejor gestión clínica por el número creciente de pacientes y es fuente de ahorro para los servicios clínicos.

# Abstract

Smart textiles with medical applications offer the possibility of continuous and non-invasively monitoring which benefit patients and doctors. To measure blood pressure in premature infants a miniature actuator that can be sewn to the fabric is required. For this reason, an actuator based on shape memory alloys has been designed so that it compresses as a conventional air cuff but with 3.5W power consumption and can be controlled by applying different Pulse-Width Modulation (PWM) signals, thus offering several levels of compression. In addition, the first concept prototype of the smart jacket is achieved; made of a natural fiber fabric that incorporates: an optical sensor, a capacitive pressure sensor with great accuracy, the force actuator and a Lilypad Simblee control board which can be sewn to the fabric, is washable and has a Low Energy Bluetooh module (BBE) to connect to other devices. All this allows the systolic, diastolic and cardiac pressure to be measured for the first time in the world with the smart jacket by a semi-occlusive method. Altogether with a mobile application which allows doctors to monitor the patient at every moment, perform remote control, data measurement and recording in a comfortable and intuitive way that satisfies the necessity for a better clinical management to the growing number of patients and is a source of savings for the clinical services.

# Acknowledgements

I like to express my grateful thank you and my sincere appreciation to the person I love more in this world. For all your disinterested help, unconditional support and for helping me through the problems with your sweetest smile and tenderness I really thank you *des del meu cor*, Rose, love of my live.

I also want to thank my project tutors from the EEBE, Xavier and Gil, for supervising my work from their knowledge and sharing with me their resources.

Anonymous UPC professors that are always willing (with previous appointment) to share their knowledge and wise advices.

Hospital Clínic, Leitat the institutions I also want to thank for their contributions.

Finally, I like to thank myself for never giving up during this long project, be visionary from the very beginning and always keep the faith until the very end.

*"… et dedico aquest petit treball per a que*
*des d'allí dalt on siguis, puguis estar*
*tant orgullós com el teu fill està de tu."*

*"Roser, darrere un punt final,*
*hi ha un espai en blanc,*
*per seguir escrivint*
*a poc a poc i amb bona lletra."*
*."*

*"Mare, germans i bestioles,*
*gràcies per creure en mi,*
*el meu èxit es també vostre"*

*"A tots us estimo."*

# List of Content

# List of Tables

# List of Figures

# CHAPTER 1:

# *Introduction*

In neonatal ICU's (Intensive Care Units), premature infants that aren't enough healthy for staying with their parents, are being monitored by the help of external medical devices like monitors and incubators 5x greater in size. Those devices, employ use and throw disposables for blood pressure measurements and had to be replaced every day for long-term monitoring because they could cause irritation on baby's skin. This also implies a high learning curve for employees because they had to deal with plugging and unplugging those devices and could end up in an accident. Further, they don't have internet connectivity features such as WiFi modules and the data have to be stored and sent by serial communication. ICU's rooms, are often full of patients and it is mainly due to the enormous amount of space required by devices surrounding the baby. Modern technologies like smart textiles that include all the necessary biosensors in a small piece of fabric, may be applied to overcome those problematics.

## 1.1. Motivation

While I was working in my internship in "La seu de Maternitat de l'Hospital Clínic de Barcelona", my tutor dr. Oscar Garcia brought me the opportunity to see the premature infants being monitored with my own eyes. The first though that came to my head, was: "Oh, god. All these tiny creatures really are human beings?" They were so small that I had to lean out of the incubator window to clearly distinguish their proportions. They were butt naked lying in the incubator alone, and covered with all type of gadgets. Electrodes, cuff in the arm, clothe strip at the finger, some of them with respirators… Surprised, I told to myself: "What is going on here?" After years of hearing my teacher in the lecture sessions explaining carefully the magic underlying the plastic cover of these medical devices I couldn't believe how exaggeratedly big they were in comparison to the baby's limbs and body dimensions. Then, I turned around and among all the nurses and staff constantly moving from one place to another I spotted a window connecting with the main hall. Baby's parents were not allowed to get in the incubator's room so they had to see everything expectantly through that window. I tried to imagine what would be a dad thinking of its baby if he would see him in that way. He would have lots of desires to have his baby safe and sound at home.

Currently, we are living in a fantastic era where custom-made solutions are possible even for the smallest patients. The need for smaller medical devices playing a key role in monitoring premature infants at ICU hospitals pushed me towards the smart textiles field. I and dr. Oscar Garcia strongly believe that a sensorial jacket that not only measures physiological data but also biochemical is no

longer a matter of fiction. My goal with this project, is to set up a starting point for smart textiles in maternity hospitals. I hope that with the design of a novel smart jacket and a novel pressure bracelet with the highest power-to-mass ratio and embedded in a fabric, it will prove the point that when size is a constraint we should use our environment and bring the technology even closer to the patient.

## 1.2. Specific aims

This TFG aims at proposing a novel smart jacket for measuring blood pressure on premature infants based on smart textiles and shape memory alloys.

**Aim #1**: To analyse the current situation of smart textiles to perform multiple physiological measurements in premature infants.

**Aim #2:** To analyse the current non-invasive methods for blood pressure measurement.

**Aim #3**: To design a compression bracelet that works as actuator based on shape memory alloy.

**Aim #4:** To build a proof-of-concept prototype of the smart jacket for blood pressure measurement.

**Aim #5:** To test *in vitro* the ability of the proposed system to measure blood pressure in premature infants.

**Aim #6:** To design a user mobile interface for control, measurement and registration of the blood pressure results.

## 1.3. Scope of the project

This project is included inside what is called "Smart Textiles" which is an emerging discipline in biomedical engineering. Hence, due to its innovative character, a complete learning process of the principles and a literature research on smart textiles was necessary for not only acquiring useful knowledge prior to the development of the prototype, but also for knowing the current limitations in order to better fit the project in what is currently possible to do.

The project had a special emphasis into measuring blood pressure in premature infants in a non-obtrusive fashion and the chosen approach had to deal with well-known constraints when dealing with baby human beings: size, security, comfort... Those were seriously considered when designing the final prototype, even to the extent of having to develop new technology. This was the case of the blood pressure actuator, which was engineered using shape memory alloys to overcome the

bulky problems associated with air pumps. Finally, the prototype was built to get advantage of the modern wireless accessibility provided by the Internet of Things, by creating a mobile application running on Bluetooth low energy technology and with lots of useful capabilities for the world of medicine.

# CHAPTER 2:

# *State of the Art of Smart Textiles*

Smart Textiles (ST) or Smart Fabrics are textiles that are able to sense stimuli from the environment, react and adapt to them by integrating new functionalities in the textile structure provided by smart materials. The stimulus and response can have an electrical, thermal, chemical, magnetic, or other origin [1] . There are mainly two categories of ST: the first one is intended to support the electronic components (off-the-shelf). In this case, wires are replaced by conductive cables and fibres. In the second category the electronic function of sensors and actuators (e.g. electric measurement of an electrode) is substituted by textile electrodes sewn into the fabric. ST that have a control unit often are referred as Very Smart Textiles.

There is an important distinction between ST and wearable devices. The later are regular fabric that envelopes traditional electronic devices. Therefore, a textile integrated wearable device that takes advantage of a textile subtract not only for support but also for functionality could be referred as Smart Wearable.

In this project a prototype following first type very smart textile will be accomplished. However, related work presented will include both first and second type of ST, and Smart Wearables in terms of providing the reader with an overview of today's market ST.

## 2.1 ST for multi-sensing

For many years now, both small start-ups and well-established corporations have been trying to increase their growth by launching their ST solutions for a wide range of applications: sports, space, medical, day-to-day, etc. They often offer biological signal sensing covering: ECG, respiratory signals, pressure, temperature, activity; and a data visualization environment on smart phones or even data storage in the cloud. In this chapter, it is presented an overview of the market situation, medical application scenarios, related work and future trends.

### 2.1.1 Market situation

Globally ST market is predicted to be USD 4.72 Billion by 2020, at a CAGR (Compound Annual Growth Rate) of 33.58 % [2]**.** It is interesting to see what are the factors that contributed to this growth over years: the miniaturization of electronic devices allowed a fastest integration into the textiles and a significance higher density of electronic components in PCB's (Printed Circuit Boards).

The manufacturing of flexible PCB allowed the board to conform a very specific shape during its wearable application thus allowing for an easiest integration and enhancing user's comfort. Also rapid growth of low-cost wireless devices, let data to be stored in the cloud and accessed at any time for application purposes or monitoring tasks. This last one relies on low-latency networks and high bandwidth for real-time monitoring which is being achieved with the release of 4G/5G/Wi-Fi networks and low-powered Bluetooth modules.

## 2.2. Medical applications

Chest belts, pulse watches, sleep shirts, fitness trackers mounted on wristbands or headbands, are some of the usual wearables available today in sports and fitness field. Not only they are increasingly being used by professional athletes but also by athletes hobbyist who want to take over their personal health. The wearables presented before, when they are compliant with medical standards and can offer reliable data and of course, are based on non-invasive measurement methods. They can perform interesting tasks such as: elderly and baby monitoring of cardiac signals by integrating ECG sensors into shirts, respiratory monitoring by knitting inductive plethysmography bands, glucose or SpO2 (Partial Saturation of Oxygen) measurements with woven optical fibers (e.g Fibber Bragg Sensors), patient tracking using RFID (Radio Frequency Identification), etc.,[3],[4],[5]. Patients who have to visit doctors on a regular basis could be overseen directly from their homes, thus creating a negative feedback between specialist and patients in real-time.

### 2.2.1 Remote Patient Monitoring

Remote Patient Monitoring (RPM) by means of the technology deployment of medical devices outside clinical settings (i.e. patient's home) for monitoring purposes plays a key role in improving patient's quality of life and benefits from low-cost solutions. Nowadays, every RPM setup must include [6] :

1. Sensors to measure physiological parameters using wireless communications standards such as: Bluetooth, ZigBee, IEEE 802.11, Wi-Fi or Low Energy Bluetooth.
2. A local data storage (cloud gateway) that interfaces sensors nodes and cloud repositories.
3. Diagnostic application software ready to send intervention alerts based on data analysis and professional opinion.
4. A cloud based repository to store data from sensor nodes, local data storage, diagnostic applications and healthcare providers.

In like manner, considering ST and the Internet of Things (IoT) for a wearable RPM deployment is a win-win situation. ST not only could be a feasible solution for the integration of off-the-shelf components, but it could also create an interface layer by using conductive threads between sensors and control units (i.e. Microcontrollers) without compromising patient's comfort. In this case sensors would be collecting valuable data and control units would be processing and acting like the local gateway to the cloud. On the other hand, IoT provide ST projects with an application platform to build user-patient interfaces for iOS or Android devices and facilitates the data flow. It also enables to manage cloud for large data storage needs and it assures that only allowed personnel will have access to the patient data.

## 2.3 Related work

Most of the ST technology available today for the sensing of physiological signals is based on physical sensors that respond to physical changes in its environment. Table 1 shows a list of the main physiological signals that might be measured using textile-based sensors.

| **Measure** | **Textile-integrated sensors** | **Source** | **Sensor Placement** | **Related projects** |
|---|---|---|---|---|
| Breathing (Breathing rate, tidal volume) | Inductive plethysmograph, Piezoresistive and strain, Impedance pneumography. | Contraction and expansion movements during volume change in breathing. | Abdominal and/or thoracic region. | [3], [4] |
| Muscle activity (surface EMG) | Textile woven electrodes. | Electric muscle activation. | Skin surface. | [5], [7] |
| Heart activity(ECG, heart rate) | Textile woven electrodes. | Electric heart activation. | Thoracic region according to different leads. | [3], [8] |
| Blood oxygen saturation | Optical fibers and optical components (LEDs, photodiodes). | Changing of IR light absorbance of haemoglobin during the pulsing arterial blood. | Earlobe or Fingertip. | [9] |
| Blood pressure | Photopletismography and ECG features, flexible pressure sensors. | Arterial pressure pulsations. | Upper arm. | [10], [11] |
| Body temperature | Textile-woven thermistors. | Body thermal radiation. | Arm, thoracic or armpit region. | [12] |

**Table 1:** Physiological signals currently being measured using smart textiles systems.

The following subsection is focused on ST projects intended for medical use on premature infants in a clinical setting and for medical professionals. Most projects fall out of the scope of sensing all physiological signals in one device but instead, they act as a separate part that could escalate to a more complex structure. As example, see Figure 1.

The Neonatal Intensive Care Unit (NICU) is a complex medical facility that aims to increase the chances of survival of critically ill premature infants and new-borns. In Figure 1, a premature infant is situated inside the incubator and connected to life-supporting devices, sensors, catheters, among others. The image illustrates the current situation in NICU's, where the amount of electronic gadgets surrounding the patient is astonishing. Measures to reduce the inherent complexity of those devices should be carried on to facilitate the task of employees, to reduce the clinical costs and to incorporate more cost-efficient and state-of-the-art technology like the Internet of Things.

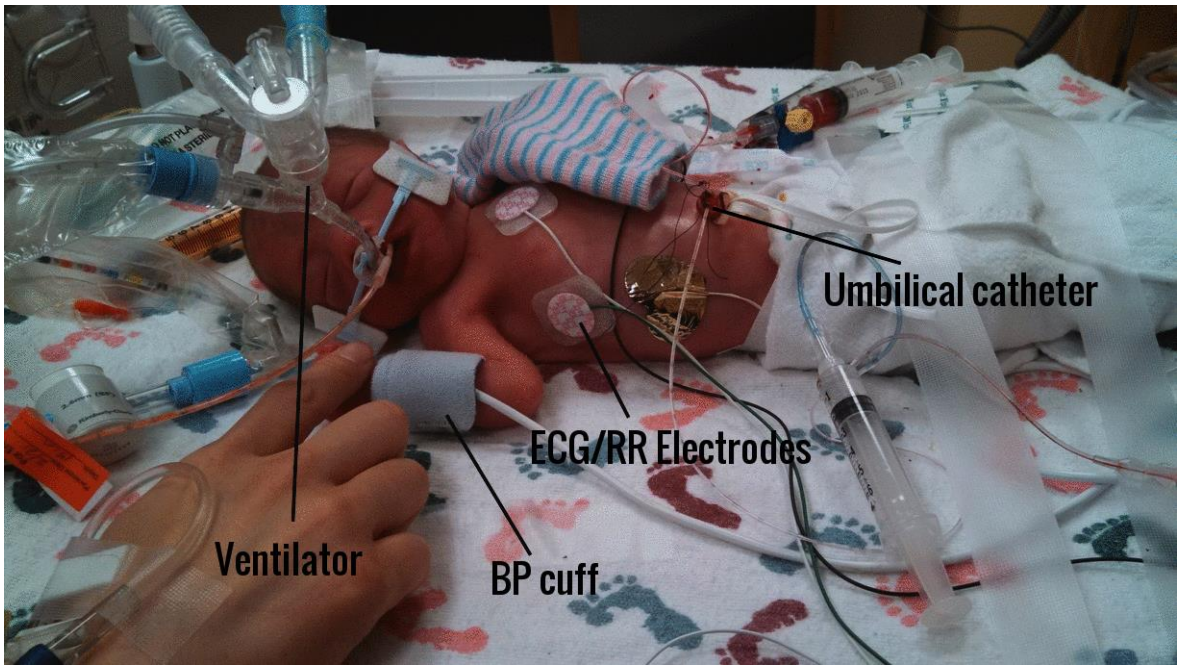


**Figure 1:** A premature infant of 28 weeks of gestation at the moment of routine check by a nurse working on a NICU [13] .

### 2.2.1 Smart Jacket for heart activity.

The work Smart Jacket Design [8] proposed a textile design for ECG neonatal monitoring by embroidering textile electrodes onto a jacket. See Figure 2. Their approach depended on proper electrode-skin contact for providing reliable data. The design process consisted of 4 steps: Information search, technological requirements, design development, which included user and

technology test, and finally a concept design validated in a clinical trial in the NICU (Neonatal Intensive Care Unit). Before applying the prototypes, they performed an analysis of risks and a wearability test on a baby manikin.

Clinical validation is an important step which could save a valuable amount of time during the design process because it receives direct feedback from the end user. However, this remains only available for the research group with professional contact to the ICUs or those that includes a healthcare professional (i.e. a doctor) in their group.

In regards to the jacket design, they came up with an open structure fabric on the back for facilitating medical observations and skin-to-skin contact therapies like Kangaroo mother care. They did not provide information on the fabric material but they made emphasis on its stretchable and flexible properties.

They developed different textile electrodes for ECG measurements according to their electrical properties. In the jacket they included 6 textile electrodes to check for the best skin-contact impedance to perform ECG measurements. They came up with 2 final approaches for the electrodes: a gold printed, and a silver plated nylon. The fabrication process consisted in building three layers: the first layer to sew the electrode, the second as a support and the third as an electrical isolation. They finally agreed that ST can offer new design opportunities like tightness on the electrode-skin contacts and comfort thanks to soft threads used to stitching electrodes. They also mentioned that their signal quality was at the level of gel-like electrodes. As they efforts were towards creating a working ECG textile electrode, they left the doors open for future research into the integration of wireless modules, as their project was working in a local environment connected to a serial port, and power supply. Therefore, they did provide an electrical consumption for assessing efficiency of the ECG measurements.

**Figure 2:** From top to bottom: Dressing process and test patches for textile electrodes [8].

### 2.2.2. Smart belt for body temperature.

In Chen et al. work [12], a ST belt capable of monitoring body temperature of new-borns was designed. See Figure 3. They used a NTC resistor (Negative temperature coefficient) fully-integrated using conductive textile wires. For building the belt, they used soft bamboo fabrics for they antibacterial, breathability and softness properties and they designed it in a straight-like shape, making it both comfortable for the baby and for the temperature measurement (the less thermal mass, the better results). They also ensured their belt could potentially be integrated into a monitoring platform or sensor jacket design like the previous work. Scalability is often a key feature for mass production and future design iterations.

The NTC resistor provided great accuracy (typically under 0.1ºC) and was easy to be integrated into the textile. In order to protect it from external factors, they electrically and thermally insulated it using soft cotton foam.

Regarding the electrical connections, they used Shieldex silver plated nylon yarns as flexible and conductive wires which proved to have higher resistance in comparison to normal copper wires. This resulted in two different resistance-temperature responses that did not affect the accuracy as this range between (37-41) ºC was not biased and showed a good linear response.

**Figure 3** From top to bottom: The designed belt and the sensor isolation using foam[12] .

## 2.3. Current and future challenges for ST

### 2.3.1. Textile techniques and materials

One of the main building blocks for ST is the sensing fabrics. This may change due to the application desired, the sensing capabilities or the textile requisites. Therefore, the main challenge is to find the proper material and processing method for allowing mass-production at low cost. Finding the right material will determine the final result. In ST designs, it must be taken into account aspects like: textile breathability, since it is necessary to have a fabric that evacuates the sweat from the skin; antibacterial properties, to control the odour and the spread of infectious microorganisms; texture, softness on the skin contact will make wearability comfortable and aesthetic (e.g. color: dyeability; resilience of the fibers). On the other hand, finding the right processing method (i.e. weaving, knitting, stitching, among others) could prove to be time consuming. As example, weave fabrics is itself a complex method. They are built onto a flat fabric surface and they have yarns running lengthwise called warp yarns and in the transverse directions called weft yarns. A weave is the pattern of yarns passing over and under each warp and weft yarns and, eventually, it will define the structure of a fabric and, in turn, its behaviour (flexibility, stiffness and ergonomic adaptation).

### 2.3.2. Electronic integration

Another challenge is the textile-electronics interface. When using sensors for monitoring physiological signals, it is desired to obtain reliable data. Therefore, the challenge is the selection and realization of the sensing function and the driving circuits integrated into the textile. The fabric should not be an impediment but act like a driving force. To obtain non-invasive data from human activity there are difficulties mainly due to the motion that cause artefacts and noisy signals, the skin that could remain unpredictable in specific settings, and signal interferences in capacitive sensing. Also for each type of sensing: bioimpedance, biopotential, capacitive or resistive; the skin-electrode contact is an important issue to be addressed if it is desired to have a clean signal without offsets or artefacts.

### 2.3.3. Energy

Energy is another major challenge when trying to integrate a sensing circuit into the textile, not only for the battery life but also for its stiffness and weight versus volume compromise. However, the future is promising, the increasing number of Li-Po rechargeable battery cells with a capacity in the range of 110mAh to 2500mAh and voltage from 3.7 to 4.2V is evolving, thus allowing ST to benefit from the reduction of frequent battery charging. Also, energy harvesting based on

piezoresistive effect could power textile-based application thanks to the repeated strain in body movements [1].

### 2.3.4. Electronic miniaturisation

ST benefits from electronic miniaturisation in the portability, size reduction and power consumption of the devices. However, sometimes small unobtrusive sensors are not available in the market or they just have not been designed yet for medical measurements (e.g. biochemical sensors) and ST must be able to cope with these challenges by designing outside parts specifically made for these components to be fitted to the design.

### 2.3.5. Wearabilities

ST must retain its functionalities over washing cycles. This is also a challenge when the electronics are not washable but they need to be integrated in the textile. To put this right, epoxies and plastic protections can be added to the circuit covering the non-washable parts. Nevertheless, this is a valid solution for most sensing devices once they are sewn and connected to each other. Control and wireless units cannot deal with permanent epoxies and therefore, conductive snap fasteners attached to the textile by sewing are used instead. Unplug on washing and plug it back for sensing.

### 2.3.6. Medical Acceptance

All sensors systems may become redundant and not successful if doctors do not want to use them in clinical settings. It is important to get the attention of medical professionals in the project for its capabilities, ease of use and to maintain and for its safety.

# CHAPTER 3:

# *Blood pressure for ST*

In this chapter the main cuffless and cuff based devices that measure blood pressure non-invasively will be explained. These technologies take advantage of being novel sensor devices which obtain blood pressure directly or indirectly from sensor data. As a detailed analysis of the clinically-relevant non-invasive techniques for the measurement of blood pressure is out of the scope of this work, their working principles and clinical acceptance will be briefly introduced.

Section 3.1 provides information about blood pressure and, specifically, about the four representative indicators of blood pressure. In Section 3.2, the cuffless measurement and the most representative technique are explained. In Section 3.3, the cuff based measurement and a semi-occlusive method are introduced.

## 3.1 Blood pressure

The force with which the human heart pumps blood to the body organs and tissues makes blood move at a certain speed. In its path, it pushes back blood vessels generating a certain pressure which is defined as blood pressure. This is a value that continuously changes as the heart is pumping blood in a cycle.

When the heart beats, it generates the systolic blood pressure which represents the highest level of pressure. When the heart relaxes between beats, it generates the diastolic blood pressure which represents the lowest level of pressure. The two values altogether form blood pressure.

Due to the beating mechanism of the heart, arterial BP is not a single value but a continuous series of values and the four most representative indicators (Figure 4) are the following:

**Systolic pressure (SYS):** the maximum value of an arterial pressure tracing.

**Diastolic pressure (DIA):** the minimum value of an arterial pressure tracing.

**Mean Arterial pressure (MAP):** the mean perfusion pressure throughout the cardiac cycle. MAP is measured as the area under the pressure curve divided by the width of the base of the pressure curve (time interval of a cardiac cycle). MAP is the most stable hemodynamic parameter because is not dependent of wave reflection. A good estimation formula of MAP when the heart rate is close to the normal values is the following:

$$MAP = \frac{SYS+2DIA}{3} \quad \textbf{(Eq. 3.1)}$$

**Pressure Pulse (PP):** the difference between SYS and DIA.

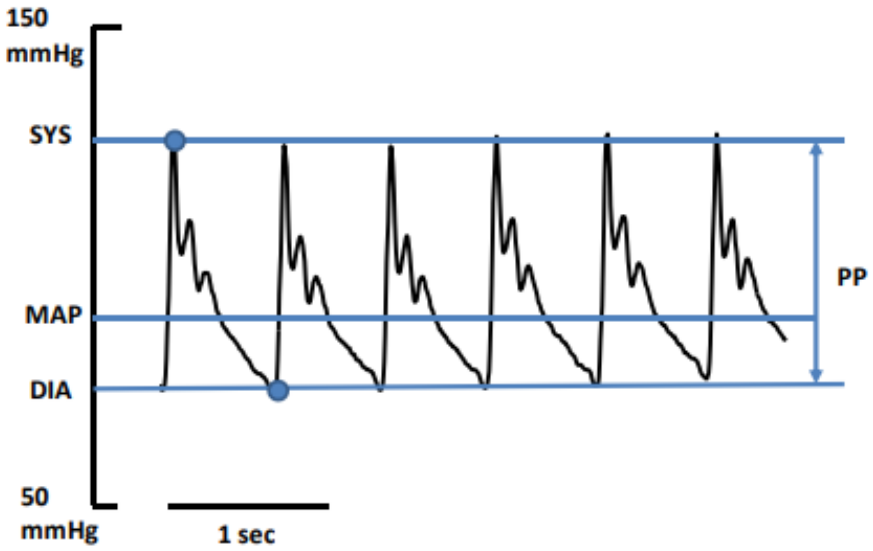


**Figure 4:** All the four indicators represented in an arterial blood pressure recorded at the finger (SYS, DIA, MAP and PP) [14].

### 3.1.1. Blood pressure thresholds in premature infants

Premature infants, are the babies whose bodies and organs aren't mature enough for working under normal physiological conditions due to having being born before completing the week number 37 of gestation, which is fixed to 280 days with 15 days offset [15] .

Premature infants can suffer from hypotension because their autonomous nervous system is unable to maintain the vascular tone, sepsis or for cardiac insufficiency . Likewise, they can also suffer from hypertension. The reported incidence in infants admitted to neonatal units suffering from hypertension ranges from 0.2-3.0% [16]. Therefore, blood pressure monitoring plays a key role in preventing morbidity and mortality rates associated with hypotension and hypertension conditions.

Normal blood pressure values in premature infants are difficult to define because they have a tendency to increase with the postconceptional age (i.e. the gestation age in weeks plus number of weeks since birth) and birth weight [17]. Studies that provide this data should have large number of samples and specify the clinical situation at the time of measurement (i.e. non-ventilated or ventilated patients, etc.) because the blood pressure readings may be affected [17].

In this project, the smart jacket aimed to measure blood pressure in premature infants. However, an interval of eligible premature infants have been defined always looking to include the largest number as possible. The interval (Eq. 3.2 and Eq. 3.3) was selected by the postconceptional age and baby weight.

$$28w \leq PA \leq 40w$$

**(Eq. 3.2)**

$$750g \leq W \leq 5000g$$

(**Eq.3.3)**

where $w$ is weeks, PA is Postconceptional Age and $W$ is the baby weight.

The lower limit of 28 weeks represents the threshold where intra-arterial catheterism can be substituted for a non-invasive blood pressure assessment. Usually this value varies with the local clinical standards and the level of criticality of the patient [15][17].

The weight limits have been selected based on the data available in the scientific literature.

The pressure range or pressure thresholds, therefore, will be determined for the selected interval of premature infants and using as a reference the study on 147 non-ventilated patients that assessed mean, diastolic and systolic blood pressure with the oscillometric method [17]. Finally, it has been determined by taking the systolic and diastolic values in the worst case scenario. Refer to Table 2 for the comparison between the normal and worst case scenarios.

| | **Systolic Pressure mmHg** | **Diastolic Pressure mmHg** |
|---|---|---|
| Normal case scenario | 53.00<br>(Centile 50$^{th}$, PA=32w) | 31.00<br>(Centile 50$^{th}$, PA=32w) |
| Worst case scenario | 76.00<br>(Centile 90$^{th}$, PA=35w, W= 3500g) | 25.00<br>(Centile 10$^{th}$, PA=28w, W= 1500g ) |

**Table 2:** Comparison of normal and worst case scenarios in systolic and diastolic blood pressure in premature infants [17].

## 3.2. Cuffless measurement

A cuffless measurement device is usually defined as the device that measures blood pressure without cuff occlusion or a pressure cuff. It takes ECG or photoplethysmography (PPG) data of the patient and feeds it to an algorithm which eventually calculates blood pressure. Nowadays, its use for diagnostic purposes still remains uncertain because certain factors such as body position or exercise might trick the algorithm and therefore, producing wrong measurements. Moreover, technically it could not be named cuff-free as most of these devices need a cuff-based device in order to do the calibration. In spite of the controversial accuracy of the pulse transit time, it is increasingly playing a key role in cuffless measurements and it will be explained in the following section.

### 3.2.1. Pulse transit time

When heart beats generate a pulse wave, which is much faster than circulatory blood speed and spreads all over the arteria and blood vessels. A technique capable of measuring the active time of the pulse wave between two determined arterial points will reflect the relative changes in blood pressure whether time increases or decreases.

Often but not always, pulse transit time or PTT is estimated as the time delay between R peak of ECG and P base point of PPG waveforms as depicted in Figure 5**.**

ECG is measured using a set of electrodes placed on the skin. These electrodes measure tiny electrical changes caused from depolarizing and repolarizing of the heart over time. PPG is measured using a set of LED and phototransistor placed in skin where capillary tissues are partially visible like in the fingertip. It measures the volumetric change of blood over time. This volumetric change measured from the periphery is not linearly correlated with arterial pressure. In addition, the signal is highly dependent of motion artefact and then, it requires a still position, training, and filtration to obtain a clean signal.

Currently, PPT still has some limitations [18], which makes medical acceptance difficult and different approaches are being investigated in order to get a better accuracy.

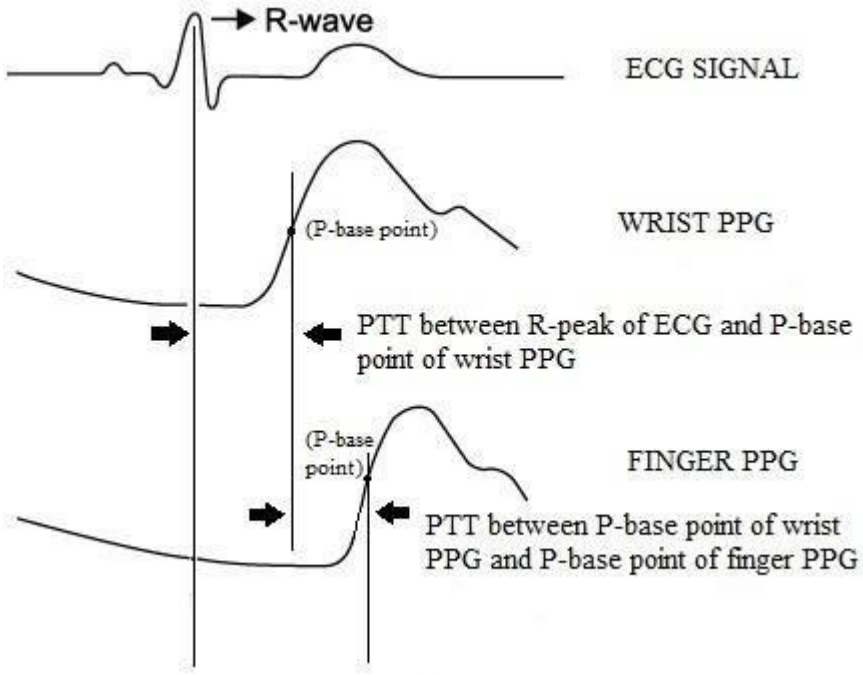


**Figure 5:** Pulse transit time estimation using ECG and wrist or finger PPG. Note that as the distance from measurement point to heart increases so does pulse transit time and that PPG shape is different depending on the sensor position [19] .

## 3.3. Cuff-based measurement

Cuff-based blood pressure measurements consist in the compression and decompression of a limb and its vasculature by encircling an inflatable compression cuff and identification of systolic, diastolic and mean blood pressure at the parameter identification points [19], [20]. The most common technique that takes advantage of cuff occlusion is based on oscillometric principle.

In opposite to cuffless measurements, oscillometric provides an intermittent assessment of blood pressure and fails to provide the hemodynamic changes of blood pressure continuously because they are subjected to compression and decompression cycles. Nonetheless, most of the devices working under this principle have been accepted for their use in non-invasive clinical practices as they are compliant with the <5 mmHg in average of blood pressure readings accuracy set by the Association for the Advancement of Medical Instruments (AAMI) [20] when compared to a centrally placed arterial catheter (gold standard).

In the following section, the engineering aspects that make possible the cuff-based blood pressure measurement will be highlighted.

### 3.3.1. Oscillometric measurement

It was born to overcome the operator-dependent nature of auscultatory methods and currently, it is an automated unsupervised device with good accuracy to measure blood pressure. The working procedure is the following. An inflatable bladder, see Figure 6, is attached to a cuff which is designed to fit the patient's arm. The bladder is then inflated by means of air injection from a conventional air pump placed in an external device which is constrained in size and power and which eventually, makes the cuff to compress. The counter pressure is then transmitted to the arm to collapse the brachial artery.

**Figure 6:** Inflatable cuff bladers. **Top**: For a 32w of gestation premature infant. **Bottom**: For a 28w of gestation premature infant. w=week [21].

The inflating cycle usually adds turbulences which are related to electrical signal noise obtained through a pressure sensor. That is one of the reasons why the measurement is performed inversely. The bladder is first inflated to a maximum range of pressure far above the expected systolic limit for the patient characteristics. Then, it is progressively deflated in a linear trajectory and oscillometric changes in the pressure pulse are evaluated together with the occluding pressure applied to the cuff to assess arterial blood pressure. Therefore, all the blood pressure features are obtained in the deflation cycle. The full measurement time results in the range of 30 to 40 seconds [22] as depicted in Figure 7.

As commented before, although oscillometric devices are clinical accepted due to its great accuracy, its drawback comes as means of patient discomfort by the long measurement time and pressure to the patient's arm applied by the cuff.

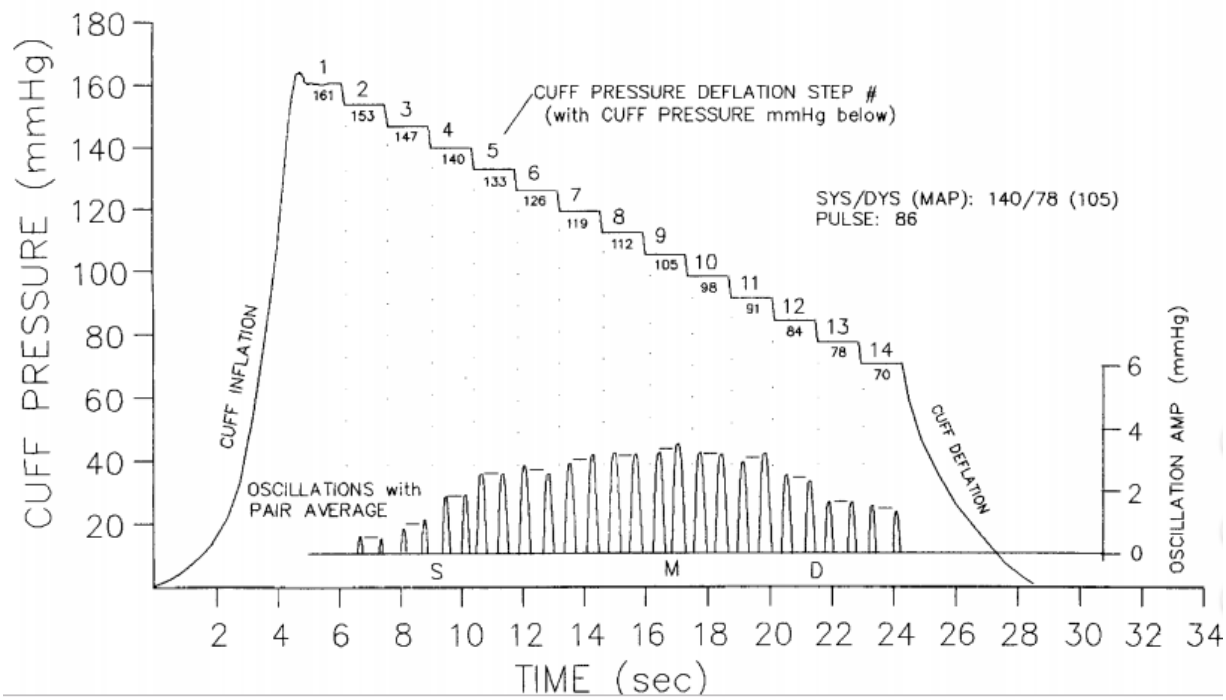


**Figure 7:** Full inflation and deflation ideal cycles necessary to perform blood pressure measurement [20] .

### 3.3.2. Semi-occlusive measurement

Semi-occlusive methods combining both cuffless technology (i.e. data obtained through PPG signal) and cuff-based technology (i.e. partial occlusion of artery or vessel by a cuff) allow a continuous noninvasively arterial pressure measurement. An example is the volume clamp method.

The pulsation of an artery reaches its maximum amplitude at the zero transmural state, i.e. when the pressure inside the artery equals the pressure of its surrounding tissues. Thus, the volume clamp technique keeps the blood volume in the finger constant by controlling the pressure exerted by a finger cuff as high as the pressure inside the artery. PPG feedbacks the blood pressure pulsatility over beat-to-beat fluctuations, therefore ensuring that the pressure generated at the cuff equals the intra-arterial pressure. The working procedure is depicted in Figure 8**.**

Despite of its continuous profile, the accuracy remains controversial as in pulse time transit. This controversial status could be attributed to the fact that performing a measurement in the finger is not clinical accepted and of course, it is not compliant with the AAIM standards. Moreover, the volume clamp method remains a semi-occlusive method, and therefore, it could lead to periods of venous congestion if it was used during prolonged time periods [23].

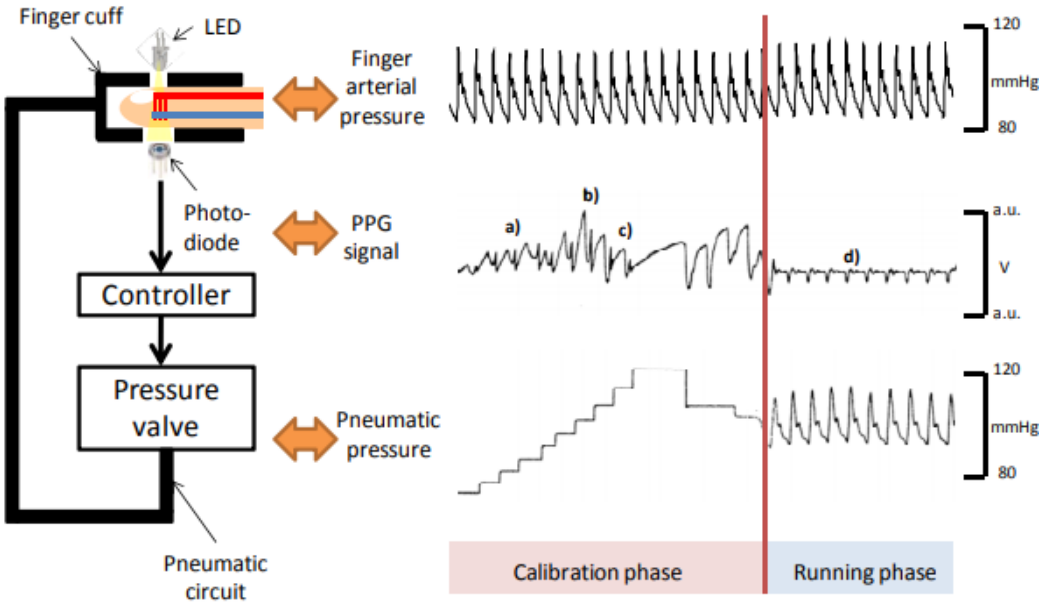


**Figure 8**: Volume clamp method for the measurement of continuous blood pressure. The Volume-clamp method to measure continuous blood pressure. Calibration phase. **a)** Cuff pressure is smaller than arterial pressure, leading to small PPG pulsatility. **b)** Cuff pressure reaches arterial pressure, leading to zero transmural pressure and thus, maximizing PPG pulsatility. **c)** The artery is collapsed. Running phase. **d)** The servo-controlling of the pressure valve continuously clamps the artery at its zero transmural state [23].

# CHAPER 4:

# *Shape Memory Alloys*

## 4.1 Shape memory effect

Shape memory alloys are unique materials that can 'remember' a trained shape under temperature drive phase transformations. Figure 9 shows the cycle that undergoes a shape memory alloy like NiTi (Nickel-Titanium). Although different combinations of alloys are available for the shape memory effect, NiTi is usually the best choice due to its stability. Nevertheless, it often turns out to be the most expensive solution.

The alloy initially presents a twinned martensite state (or elongated state) and when a weight is loaded, it changes its crystalline structure into the same martensite but in de-twinned state. The alloy could be driven into a non-reversible plastic deformation but, as far as the stress is lower than the critical stress, its original shape can be reverted by means of external heat activation. Likewise, when heated above the starting austenite temperature, not only it would recover the initial 'remembered shape' but if it was constrained during the transformation it would also produce a force. Finally, it would go back to martensite twinned state by employing effective cooling and thanks to an initial tensile strength.

The process of deformation and shape recovery can be repeated many times, and this offers the possibility of using shape memory alloys in continuous blood pressure measurements. In addition, it could be used for long-term monitoring purposes but it cannot be deformed to high strains as its lifetime could be shortened.

What makes shape memory alloys really appealing is that they can effectively achieve high forces with the lightest set-up. In other words, it has a great potential as miniature actuators and, opposite to bulky servo motors or air pumps, it facilitate the integration.

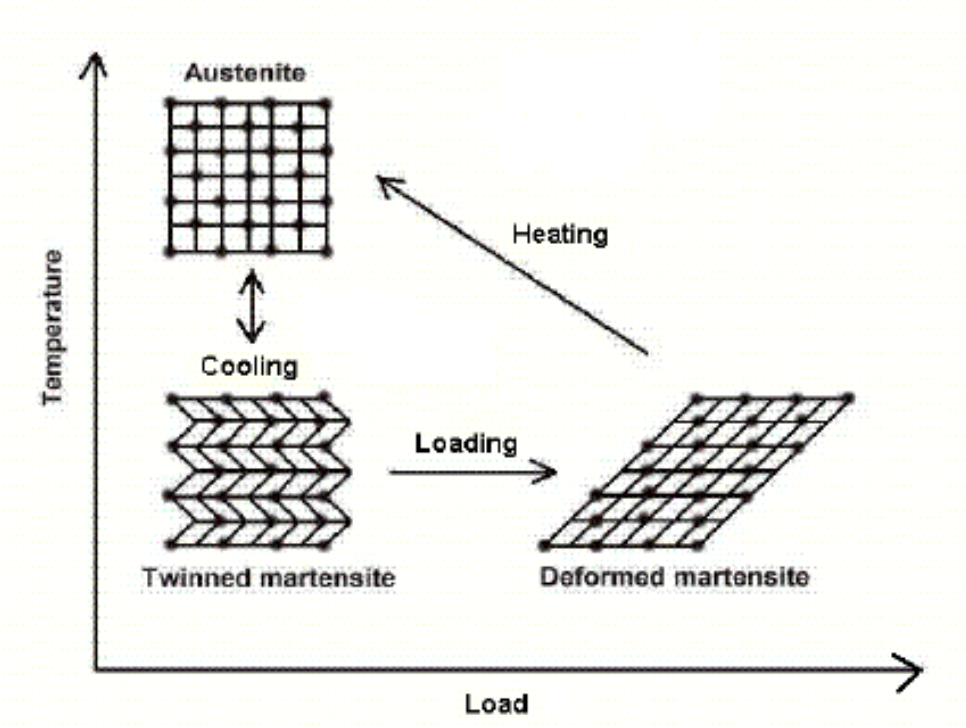


**Figure 9:** Typical phase-transformation cycle of shape memory alloys [24].

There exist different thermo-mechanical treatments in order to give a preferred shape to shape-memory alloys. The sample is heated well-above its austenitic transition temperature and hold in the preferred position while it is submitted to constantly heat and cooling cycles. In addition, the transition temperature which is subjected to the thermo-mechanical treatment is often a tuneable parameter for shape-memory alloy actuators.

Finally, one of the problems encountered when using shape-memory alloys appears when this is used to precisely predict position control. A typical stress-strain curve is depicted in Figure 10. It has a very dependent behaviour on temperature as well as on stress, which eventually results on a hysteric response.

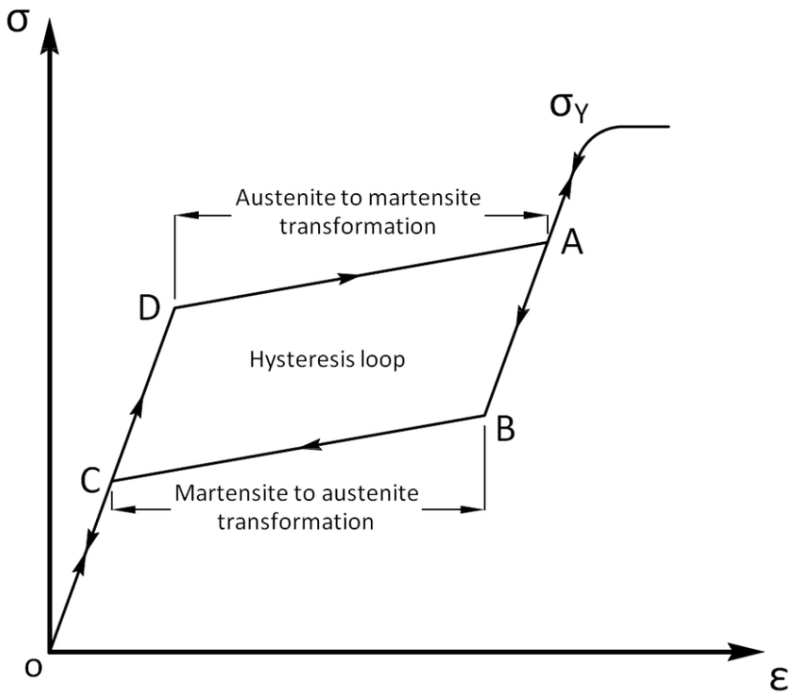


**Figure 10:** Stress to strain curve. Hysterical response [25]**.**

## 4.2 NiTi properties

The shape memory alloy chosen as micro actuator has been nitinol or NiTi. Its content typically is 55-56% Nickel and 44-45% Titanium. Like most active materials, it has a long list of transformation, physical, mechanical, electrical and magnetic properties. It is world-wide commercialized under the name of Nitinol or Flexinol wire by Dynalloy, Inc where one could refer to for evaluating the aforementioned properties [26].

## 4.3 Spring manufacturing and geometry design

SMA wires produce high recovery forces at the price of having low strokes [27]. This can be addressed if the alloy is heat-treated and shaped as a helical spring. Ultimately, the spring will form a compressed spring in their heat-activated austenitic state but the recovery forces will be reduced.

NiTi helical compression springs are defined by multiple geometrical parameters that might vary depending on the application. First, the wire diameter d. As remarked at the NiTi properties table, the electrical properties (i.e. resistivity) are exclusively dependent on the diameter. The wire is coiled using a specific mandrel size or inner diameter$D_i$, a pitch p defined as the distance between two consecutive coils, a coil angle α , a number of active coils $n_a$ and is given an initial length $L_o$.

All the aforementioned parameters are depicted in Figure 11. Mean diameter is calculated as the mean value of the inner diameter and the outer diameter.

$$D = \frac{D_i + D_o}{2}$$

**(Eq.4.1)**

And the coil angle:

$$\alpha = tan^{-1} \frac{p}{\pi D}$$

**(Eq.4.2)**

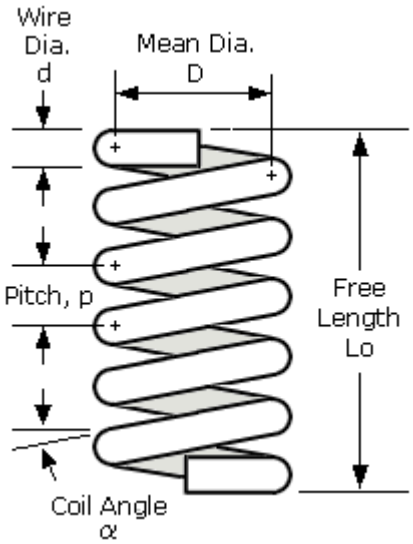


**Figure 11**: Free-length spring with closed ends and 5 numbers of active coils [22]**.**

The effect of the end treatment must be taken into account in the design process because it influences the contact area with the base [28]. Likewise, the number of active coils $n_a$, spring free $L_o$ length, spring solid length $L_s$ and pitch $p$ are derived by the module based on the specified end type. In this work, a closed end will be considered for both the testing and the design and, therefore, its corresponding formulas will be presented.

## 4.4 Force modelling of nitinol springs

The force produced by a single NiTi helical spring (i.e. $n = 1$) when this is heat-activated can be expressed in terms of its geometrical parameters, the modulus of rigidity $G$ in the austenitic state, and the Hooke's Law:

$$F = k\delta_S$$

**(Eq. 4.3)**

where according to EN-13906-1: 2013 for helical compression springs:

$$k = \frac{G \cdot d^4}{8 \cdot D^3 \cdot n_a}$$

**(Eq. 4.4)**

$\delta_s$ is the active extension and $n_a$ the number of active coils.

When substituted to Eq. 4.3 the following expression is obtained:

$$F = \frac{G \cdot d^4}{8 \cdot D^3 \cdot n_a} \cdot \delta_S$$

**(Eq. 4.5)**

As the maximum force is desired, the combination of the variables in ratios can be useful as shown in [29]. In their model, three non-dimensionalised parameters: packing density $\eta$; defined as the ratio of the solid spring length $L_s$ to the free spring length $L_o$ or equivalently, the solid spring pitch, which is equal to $d$, to the free spring pitch $p$; actuator extensional strain $\epsilon$, defined as the ratio of spring displacement $\delta$ to free spring length; and spring index $C$ defined as the ratio of mean diameter $D$ to wire's diameter $d$. The three ratios formulas are found below.

$$\eta = \frac{L_S}{L_o} = \frac{n \cdot d}{L_o} = \frac{d}{p}$$

**(Eq. 4.6)**

$$\epsilon_s = \frac{\delta_s}{L_o} = \frac{L_f - L_o}{L_o}$$

**(Eq. 4.7)**

$$C = \frac{D}{d}$$

**(Eq. 4.8)**

If the force formula is expressed in terms of the three ratios, the following expression is obtained:

$$F = \frac{G \cdot d^2}{8C^3 \cdot \eta} \cdot \epsilon_s$$

**(Eq. 4.9)**

This model explains quite well a design where the spring is stretched to its limit extensional strain and when the transformation begins. Assuming a full transformation of austenite linear region, the compression produces a force in opposite direction to the stretching force. However, in this model, it is assumed that the wire's diameter $d$ and spring's free length change due to the fact that phase transformation is negligible. However, these assumptions were justified elsewhere and it was concluded that the model is effective at predicting active forces at extensional strains up to $\epsilon_s \leq 2$ [30]**.** As full austenite phase transformation is assumed, the austenite modulus of rigidity is a constant value.

Maximum force per spring actuator is obtained when $\epsilon_s$ and $d$ are maximised, and $C$ and $\eta$ are minimised. The knowledge of the limits for both maximum and minimum values is crucial for a practical design. Therefore, $d$ cannot exceed too much in value as the current must be limited for safety concerns and for power efficiency.

The lesser spring index $C$ is, the more similar to a fiber will be, and it will also not be bulky to wear. However, in practice, this index is recommended to be higher than 3 to avoid cracking or spring damages. It is also important to know that $\eta \; and \; \epsilon_s$ are physically coupled. This means that when $\epsilon_{max}$ decreases $\eta_{min}$ decreases. Therefore, a trade-off must be considered between maximum force provided by $\eta_{min}$ and best donning for wearing provided by $\eta_{max}$ to fulfill both requirements.

## 4.5. Pressure modelling of NiTi springs

For the modelling of the target systolic (i.e. pressure $P_{sis}$ and diastolic pressure $P_{dia}$ ) it will be modelled a bracelet of width $w$ wrapped around a thin-walled cylinder of radius $r$ by the action of a tension force $T$. The relation between these variables is the thin-walled hoop stress equation or Laplace law visually depicted in Figure 12.

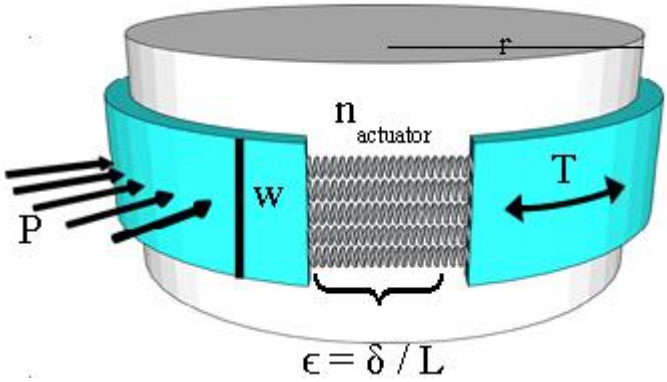


**Figure 12**: Squeezing bracelet using SMA and representation of hoop stress law[30] **.**

Variables that determine the counter-pressure applied by $n$ Ni-Ti actuators based on the general hoop stress equation under a thin-walled solid surface assumption [29] .

$$P = \frac{T}{w \cdot r}$$

**(Eq. 4.10)**

This equation is valid when the number of actuators is $n = 1$. The counter pressure generated increases linearly with the number of actuators in parallel.

$$P = \frac{T \cdot n}{w \cdot r} = \frac{F \cdot n}{w \cdot r}$$

**(Eq. 4.11)**

In order the bracelet to perform a full blood pressure measurement, it is required that the NiTi springs provide both systolic and diastolic forces to produce the target pressures. As the spring will remain the same, the only parameter that will increase or reduce force linearly is the deformation as seen in Eq. 4.11. Eventually, the deformation will be a function of the current pulse width and duty cycle exerted to the spring, duly controlled by the microcontroller.

### 4.5.1. Arm diameter

To perform the pressure modelling, it is important to determine a value for the cylinder diameter which in the human body would correspond to the Mid Upper Arm Circumference or MUAC. The assessment of the MUAC is based on an anthropometric study conducted by [31]**,** in which a set of

data was collected from a total of 209 premature infants ranging in weight from 700 g to 3500 g. Results are depicted in Figure 13.

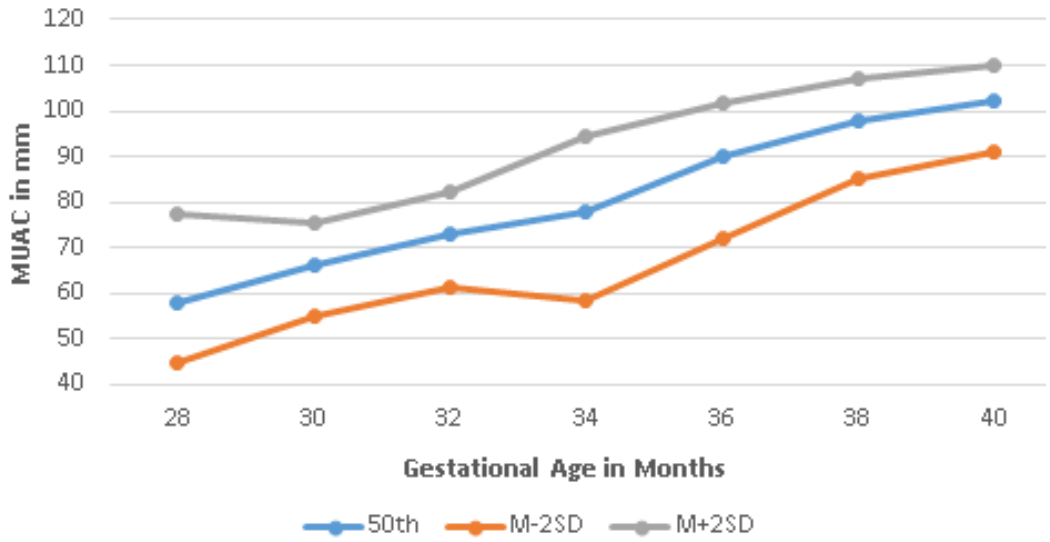


**Figure 13:** MUAC vs Gestational age of 209 premature infants ranging in weight from 700 g to 3500 g [31].

As seen in Figure 13 the MUAC ranges from 60 mm to 100 mm, which using the perimeter formula of a circle represents a diameter of the arm in the range between 19 mm to 32 mm. The diameter of the arm linearly decreases as MUAC decreases, but when the arm's diameter decreases the higher is counter pressure as seen in the hoop stress equation. Therefore, it is not only necessary to provide the targeted pressure in small diameters, which apparently would come more easily as the NiTi springs force required is lower, but the pressure at higher arm diameters must also be satisfied, which would require higher activation forces.

### 4.5.2. Bracelet width

According to the AHA (American Heart Association), a bracelet width to arm circumference ratio of 0.4 is recommended. In other words, the axial width $w$ must cover the 40% of arm circumference. Also, the bracelet length $B_L$ has to be between 80 to 100% of the same arm circumference [32]. By satisfying these two designing constraints, a more accurate measure is likely to be obtained.

$$\frac{w}{2\pi \cdot r} \approx 0.4\,; \quad B_L \in [0.8, 1] \cdot 2\pi \cdot r$$

**(Eq. 4.12)**

In addition, the bracelet total axial width will constrain the number of parallel NiTi springs in a single-layer assumption as means of the spring index $C$ and the wire diameter $d$.

$$w \geq (D + d) \cdot (n_{spring}) = d(1 + C) \cdot (n_{spring})$$

**(Eq. 4.13)**

The number of springs will be determined *a priori* as total deformation $\epsilon_s$ needed to exert the maximum force divided by a consistent extensional strain $\epsilon_{Smax}$ across all springs. The value of $\epsilon_{Smax} \approx 3$ will be taken from [29], where it was obtained for a similar application.

### 4.5.3. Pressure estimation

Finally, the active and passive counter pressure generated by n parallel NiTi springs will be modelled based on the spring-model parameters as seen in the previous chapters and the Laplace law.

| Parameter | High pressure profile | Comments |
|---|---|---|
| $C$ | 5.8 | |
| $d$ | 0.5 mm | |
| $G_A$ | 25 GPa | Reference: [29] |
| $\eta$ | 1 | |
| $\epsilon_{max}$ | 2 | Model linearity limit. Nevertheless, it could be stretched to 300% of its initial length. |
| $n_a$ | 1 | |
| $r$ | 16 mm | This value might be variable as the range of premature infants are from 28-40 weeks of gestation. |
| $w$ | 32 mm | See below for the calculus. |

**Table 3**: List of parameters used for the pressure estimation of the NiTi spring.

It is important to take into account that as the bracelet is being designed to measure blood pressure in premature infants aging from 28 to 40 weeks of postconceptional age, an optimal bracelet width must be found between $w_{28}$ and $w_{40}$ because it will remain constant in the final design. However, the axial length could be adjusted for the different arm diameters with a special closing mechanism (i.e. snap buttons or hook-and-loop). Hence, two different width obtained as the 40% of MUAC were averaged.

$$w = \frac{w_{28}(calculated\ as\ 0.4 \cdot MUAC_{28}) + w_{40}(calculated\ as\ 0.4 \cdot MUAC_{40})}{2} = \frac{24 + 40}{2} = \\ = 32\ mm$$

**(Eq. 4.14)**

A calculation of the active pressure using the following equation is provided:

$$P = \frac{T \cdot n}{w \cdot r} = \frac{F \cdot n}{w \cdot r} = \frac{G \cdot d^2 \cdot \epsilon_s \cdot n}{8C^3 \cdot \eta \cdot w \cdot r} = \frac{25000 \cdot 0.5^2 \cdot 2 \cdot 1}{8 \cdot 5.8^3 \cdot 1 \cdot 32 \cdot 16} = 15.6\ kPa$$

**(Eq. 4.15)**

The active pressure top limit is 12 kPa, but it is necessary to ensure that the artery is fully collapsed; therefore the maximum active pressure should be above 12 kPa. Likewise, 15.6 kPa in Eq. 4.15 is a good top pressure value.

Ultimately, to simulate the full range (i.e. no pressure to top pressure), a model that simulates the passive pressure exerted by the bracelet should be presented but such a model was not found in the literature. Therefore, it will be assumed that the passive pressure will fall below the diastolic pressure and the bracelet will be capable of increasing the pressure from that point to the top limit or systolic pressure.

## 4.6. Thermal modelling of NiTi springs

SMA is a smart material that actively responds to temperature changes. The increasing of temperature for the phase change of the NiTi springs is mainly achieved through Joule's heating defined as the heat in watts generated when electrical current passes through a resistor. The decreasing of temperature is mainly obtained through heat convection with the surrounding environment.

The goal of this chapter is to assess which would be the best transition temperature in terms of energy efficiency and to define the current amplitude value during the full blood pressure measurement. The general statement is that in an activation process, where a heating of the spring is required in order to obtain a change of the phase at a specific transition temperature, the higher variation of temperature (Eq. 4.16) the more time $\Delta t$ (and therefore energy) is needed for keeping the current $I$ running through the wire at a constant rate for obtaining the same extensional strain.

$$\Delta T = (A_s - T_\infty)$$

**(Eq. 4.16)**

where $A_s$ is the austenitic transition temperature.

The heat transfer theorem states that heat transfer can occur by means of three fundamental mechanisms: conduction, convection and radiation. Conduction is presented in terms of conductive heat flow to the spring (i.e. Joule's heating provided by the power connections), convection in terms of convective heat loss to the environment (i.e. natural convection) and radiation in terms of radiation heat loss. Therefore, assuming a wire form of the NiTi spring exposed to surrounding air, no radiation heat losses and heating by a constant current, the equation takes the form expressed in Eq. 4.17.

$$\frac{I^2}{A^2} \cdot \rho_{SMA}(T) = \frac{P}{A} \cdot h_c(T) \cdot [T(t) - T_\infty] + C_v \cdot \frac{\partial T}{\partial t}$$

**(Eq. 4.17)**

$$\rho_{SMA}(T) = \frac{R(T) \cdot A}{l}$$

**(Eq. 4.18)**

$$A = \frac{\pi \cdot d^2}{4}$$

**(Eq. 4.19)**

$$P = \pi \cdot d$$

**(Eq. 4.20)**

,

where $I$ is the current magnitude, $\rho_{SMA}$ is the spring resistance as function of temperature defined in Eq. 4.18, $A$ is the cross-sectional area defined in Eq. 4.19, $P$ is the perimeter of the wire cross-section defined in Eq. 4.20, $h_c$ is the heat convection coefficient as function of temperature, $T$ is the spring temperature as a function of time, $T_\infty$is the environment temperature and $C_v$is the heat capacity of NiTi at constant volume.

The heat convection as a function of temperature and diameter it will be modelled as shown in Figure 14.

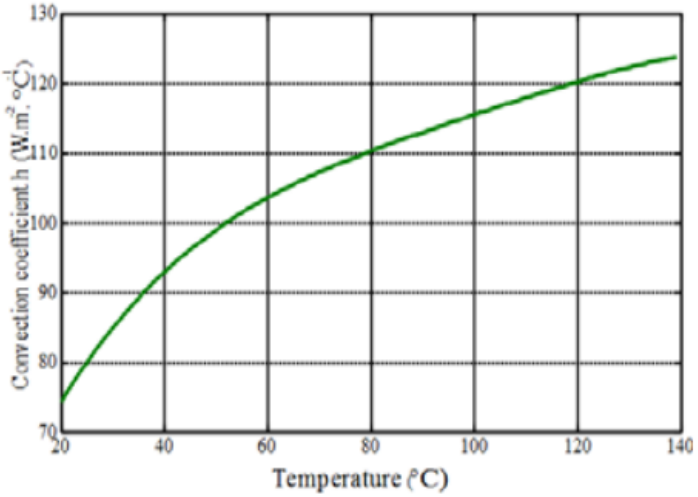


**Figure 14**: Convective heat transfer coefficient of SMA wire versus temperature[33] .

As the NiTi undergoes a phase change during transformation, its electrical properties (i.e. electrical resistivity) and heat capacity change in a hysteric form with temperature [27] which was disregarded in the equation for simplification. Therefore, the averaged values of resistivity and heat capacity of martensite and austenite will be considered to account for the temperature dependence.

It is important to note that the superelastic effects of NiTi will also be neglected, which would linearly increase the temperature when the alloy is subjected to a stress load. Assuming a constant length of a NiTi thin wire, the rearranged equation for $T(t)$ is shown in Eq. 4.21.

$$T(t) = \rho \cdot I^2 \cdot d \cdot \frac{(e^{\frac{-4 \cdot h_c(T)}{d \cdot C_v} \cdot t} - 1)}{4 \cdot h_c(T) \cdot A^2}$$

**(Eq. 4.21)**

This last equation is also useful for determining the current magnitude necessary to obtain a final temperature. As $C_v$ does not affect the final temperature (its value is maximum) the equation can be solved for I as seen in Eq. 4.22.

$$I = \sqrt{\frac{4 \cdot h_c(T) \cdot A^2 \cdot (T_{final} - T_\infty)}{\rho_{SMA} \cdot d}}$$

**(Eq. 4.22)**

For assessing the shape of the heat transfer equation, the relation will be plotted in Figure 15 and Figure 16 giving the values shown in Table 4.

| Parameter (Unit) | Value | Source |
|---|---|---|
| $d\ (m)$ | $0.5\ \cdot 10^{-3}$ | Spring used in testing. |
| $\rho_{AM}\ (\mu\Omega \cdot m)$ | 0.79 | [26] |
| $A\ (m^2)$ | $1.96 \cdot 10^{-7}$ | Calculated, Eq. 4.19 |
| $T\ (ºC)$ | 55 | The T limit was set experimentally for the given spring. |
| $T_\infty (ºC)$ | 25 | Ambient temperature. |
| $c_v\ (J/(m^3 \cdot ºC))$ | $2.05\ \cdot 10^6$ | [33] |
| $h_c\ (W/(m^2 \cdot ºC))$ | Figure 14 | [33] |
| $I\ (A)$ | 1.1 A | Figure 15 for T final=55ºC |

**Table 4:** List of parameters and values.

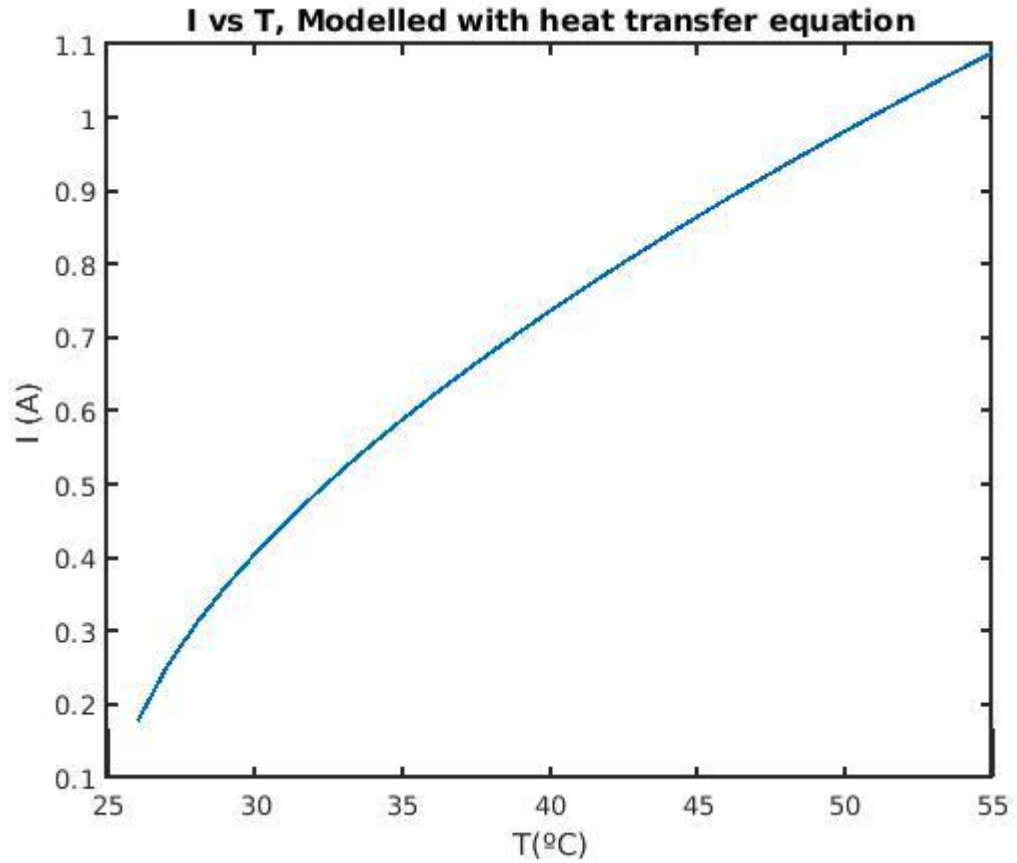


**Figure 15:** Electrical current versus spring temperature from values in Table 4. From 25 to 35 $^{o}$C the response is non-linear mainly due the NiTi warm-up.

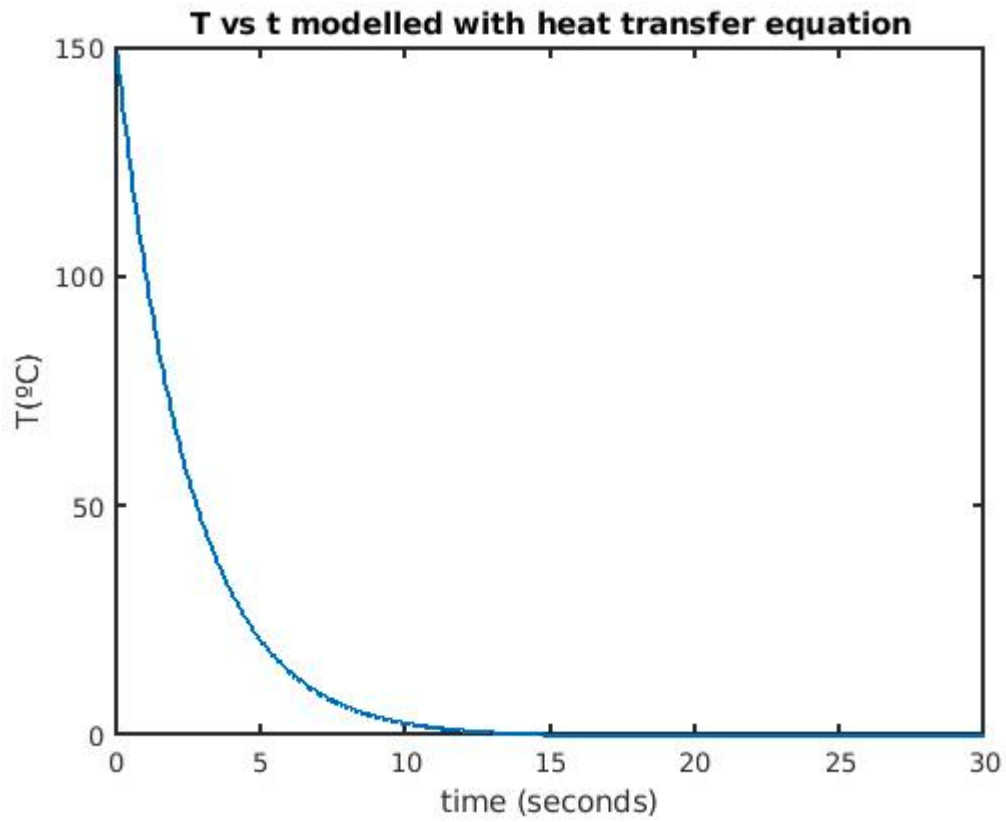


**Figure 16**: Spring temperature versus time obtained from values of table and heat transfer equation. In approximately 3 seconds the spring would go from 55ºC to 25ºC thus, indicating that the cooling is a quick process.

# CHAPTER 5:

# *Design and fabrication of the bracelet*

In this chapter, the steps for the conception and fabrication of the bracelet will be explained. Across the designing iterations that have followed the conception of the final bracelet, two final designs were selected for further experimentation which are detailed in this chapter. During the designing process, it was always looked for a simple design made of off-the-shelf components and budget-friendly. The design was divided in three main parts, each of them fundamental for the desired performance. Fabric selection, integration of the spring, and user protection.

## 5.1. Fabric selection

Firstly, the fabric selection required a wide understanding of the current fabric structures. As the time was limited, it was decided to find a certificated medical fabric for compression applications. Three different fabric structures (Figure 17, Figure 18 and Table 5) were obtained from Baltex UK [34].

| Nº | Fabric structure | Description | Properties |
|---|---|---|---|
| 3885 | 4XD | Polyamide yarn on the outer surface and Skinlife with Lycra on the inner surface. | Thickness: 3.5mm<br>Weight: 420 g/m2 |
| 3250 | 4XD | 100% Polyester | Thickness: 2.5mm<br>Weight: 400g/m2 |
| NPD 179 | 4XD | Polyester with lycra and with infra-red yarn. | Thickness: 2.9mm<br>Weight: 420g/m2 |

**Table 5:** Baltex 4XD fabric structures description and properties [35].


**Figure 17:** Three fabric structures available.

**Figure 18**: 4XD elastomeric structure. The micro elastomer filaments sandwiched between the two surfaces. This structure allows the fabric to move in the three directions with a certain elasticity.

All three share a common structure (i.e. 4XD or 4 way stretch spacer fabric) made of knitted fabrics. This type of structure ensures equal pressure distribution along all the surface, which is of vital importance, otherwise the fabric properties could incur variations in the blood pressure values on the subject [36]**.** What differentiates them is the presence of lycra, which eventually determines the stretching performance and fabric thickness. The model 3885 was finally selected because it adapts to soft feeling at skin and it was the thickest. This fact is important for the user protection and facilitated the sewing of buttons and the conductive thread.

The limitation that all three fabrics presented is the presence of polyester yarns. Generally, natural fibers like cotton or bamboo are preferable to synthetic yarns like polyester for skin contact applications, because they prevent skin irritation increasing breathability in sensitive-skins. Nevertheless, this could be solved by placing the bracelet on a cotton sleeve instead of on bare arm as there is no significantly difference in measuring blood pressure [37].

## 5.2. Integration of NiTi spring

The integration of NiTi springs on the fabric is not an easy task. Many aspects had to be considered before reaching something useful. Spring placement in the fabric structure, method of fixation, positive and negative leads, initial and final elongation, the behaviour when wrapped around the arm, thermal and electrical insulation, etc.

### 5.2.1. First prototype

The designing of the first prototype was motivated by the HapticClench project [38]which simply consisted of a NiTi spring connected via crimps to a hook and tied around the user wrist.

The dimensions were set according to the size constraints and AHA recommendations. A square shape of 3885 Baltex UK, medical fabric was taken and given a rectangular shape of 90 mm long by 35 mm wide. A layer of Kapton tape was placed on the fabric surface for electrical and thermal insulation purposes. Then, 20 mm long NiTi spring from Kellogg's Research Labs USA, 2.4 mm mandrel, 0.5 mm wire diameter and 0.5 mm pitch were placed lengthwise along the fabric surface and both end loops were sewed using stainless steel thread of 1 mm of diameter. Before sewing, the spring was stretched to 60 mm and never exceeded the 200 % deformation limit. When the spring was properly reinforced to the fabric, two male 8 mm snap buttons were sewed to the fabric using conductive thread and a conductive path was sewed to each of the spring's ends, which were previously sewed to the fabric. Hook and loop tape was firstly considered for the closing mechanism, but finally, it was disregarded because it had a poor quality over cycles of use and it could cause irritation on sensitive skins. The conductive threads were insulated using transparent epoxy and cotton thread covering the exposed parts. Figure 19, Figure 20 and Figure 21 shows the first prototype and Table 6 provides the list of materials.

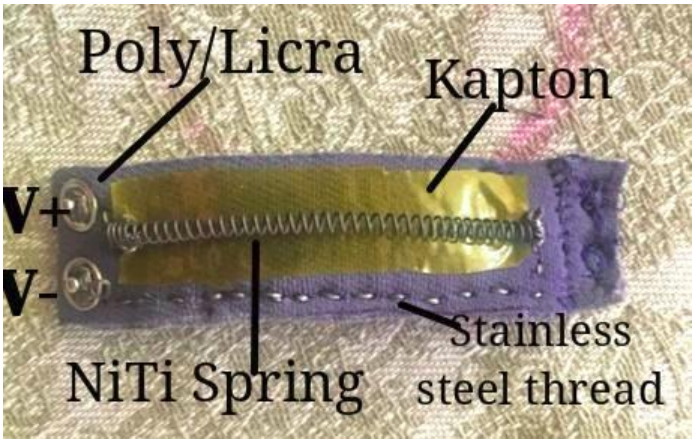


**Figure 19:** Top view of the first prototype with the most relevant parts highlighted.

**Figure 20:** Back view of the first prototype.

**Figure 21:** First prototype wrapped around the baby manikin right arm

.

| Nº | Material |
|---|---|
| 1 | 3885 4XD fabric |
| 2 | 2 male 8 mm snap buttons |
| 3 | 2 female 8 mm snap button |
| 4 | Stainless steel thread |
| 5 | Kapton tape |
| 6 | 20 mm long 0.5 mm diameter wire NiTi spring |

**Table 6:** List of materials used in first prototype.

### 5.2.2. Second prototype

Substantial changes were introduced to the spring of the second prototype. The fabric was cut to the same rectangular shape and 15 mm long 0.25 mm pitch, 0.5 mm mandrel and 0.25 mm wire diameter NiTi spring was used as actuator. The reason to choose such tiny microspings was the need to insert them in a 2mm PVC tube for total electrical and thermal insulation. A thicker tube would make the wrapping of the bracelet difficult and cause the patient discomfort. Likewise, it was

necessary to design the tube structure by the hand of CAD (See Annex B) for a better representation. This mechanism is depicted in Figure 22**.**

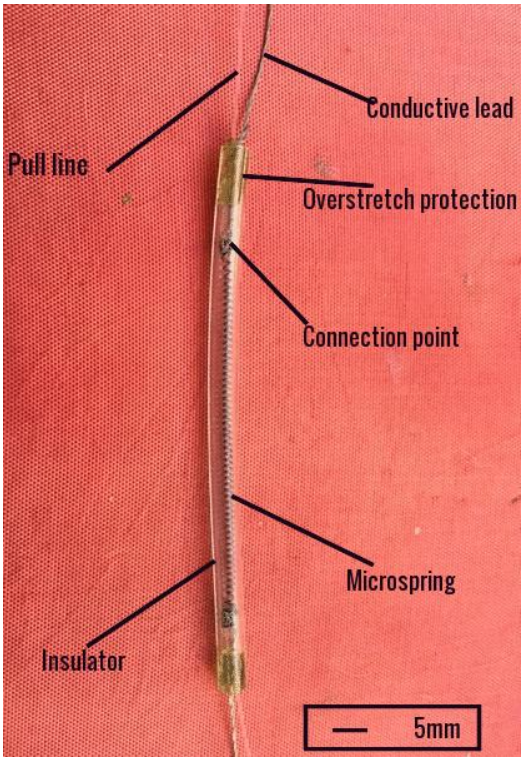


**Figure 22**: Tube mechanism with most relevant parts highlighted. The tube length is 60 mm.

Two lines interconnect the microspring from the outside to the inside part of the tube. The pull line is a 0.35 mm diameter nylon wire with tension strength of 125 N. It is connected between a pair of two snap connectors, where it is tied, and the microspring connection point. To securely tie a knot, the pull line was guided through the microspring hole and the head was removed at the fourth loop. It was important that the knot never exceeded 2 mm in height and width; otherwise it would have created an undesired friction force to the walls of the tube. The second line is a stainless steel thread that acts as a conductive lead from the voltage source. It was firstly intended to use the same line for pulling and conductive lead but the stainless steel thread was made of twisted microfilaments of stainless steel and, those would often split and cause the wire to be floppy. Therefore, it was proposed to separate both functions in two lines. When the lines were attached to the microspring, the whole structure was placed in a 60 mm long, 2 mm diameter PVC tube to act as a coating. Finally, a overstretch mechanism that not only ensured the microspring would never exceed the 200 % deformation limit which would cause permanent damage to it, but also it forced the microspring to move around within the tube.

A cotton fabric and a double backstitch were stitched on the fabric surface in order to force the tube movement lengthwise and cover the whole mechanism. The sewing machine was a JUKI MO-6700 series (Japan). Then two conductive snap connectors were sewed to the fabric using cotton thread and the conductive lead was connected to the microspring. A third snap connector was placed in between and the pull line was tied to it. Initially, the mechanism was capable of holding 4 microsprings lengthwise but, finally, we chose the configuration shown in Figure 23, with a 2 microspring configuration. This configuration is similar to a series connection of two variable resistors wired by the conductive lead (see Figure 24).

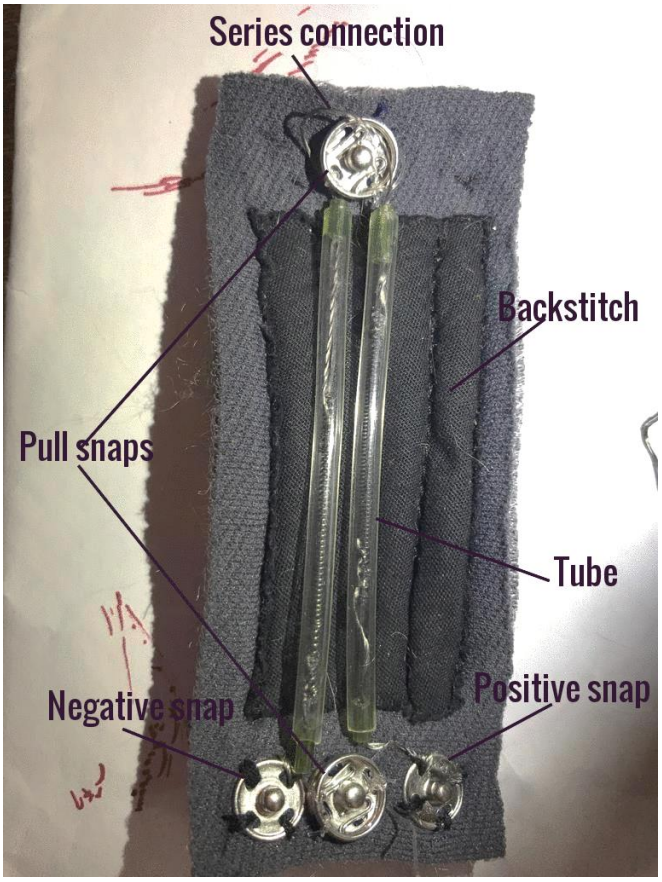


**Figure 23:** Second prototype with the most relevant parts highlighted. The springs were uncovered from the backstitch for illustration purposes but in practice, they would be placed inside the backstitch.

**Figure 24:** Detail of the series configuration between two microsprings.

**Figure 25:** Second prototype next to a 20 cent coin to illustrate its proportions.

**Figure 26:** First (left) and second (right) prototype.

| Nº | Material |
|---|---|
| 1 | 3885 4XD fabric |
| 2 | 6 male 8 mm snap buttons |
| 3 | 6 female 8 mm snap buttons |
| 4 | Stainless steel thread |
| 5 | 2 mm inner diameter PVC tube |
| 6 | 2 x 1 mm inner diameter PVC tube |
| 7 | Nylon line |
| 8 | Black cotton fabric |

**Table 7:** List of materials employed in the second prototype.

## 5.3. User protection

The patient who is going to wear the bracelet has to be protected at each moment of the measurement. Typically, this is compulsory in the creation of medical devices as stated in 93/42 ECC directive and the FMA (Failure Mode Analysis). The creation of a medical device is out of the scope of this project; nevertheless, each of the prototypes presented in this work will include a discussion of the potential risks and measures taken in each of the prototypes, because they will inherently get in touch with human beings.

In Table 8, is summarized the main potential risks the patient might be subjected to when wearing the bracelet and the actions adopted in each design.

| Risk | Source | Actions in 1st pro. | Actions in 2nd pro. |
|---|---|---|---|
| Electric shock | Conductive thread in contact with patient's skin. | Conductive threads present in the bottom surface are covered with a sewed cotton thread. Conductive threads present in the top surface are covered with transparent epoxy. Hardware ( mosfet integrated board) limitates maximum current supplied to the spring. | Same as 1st prototype but including an insulating PVC tube to cover the spring area. |
| Skin burning | NiTi spring when heat activated and/or fabric burning when | A 0.1 mm layer Kapton tape specially made for thermal | Insulating PVC tube for each spring and cotton backstitch for |

| | | | |
|---|---|---|---|
| | current is drawn. | insulation is placed at the top surface covering the whole spring area. The fabric top and bottom surfaces are also separated by 2mm polimeric filaments with empty space filled with air, therefore difficulting thermal conductivity. | thermal insulation. |
| Poor blood circulation and skin pain | Excessive and/or unevenly pressure. | Certified medical fabric ensuring even pressure distribution on the arm. A software implemented algorithm also sets the maximum amount of current supplied to the spring and the PWM duty cycle. | Same as 1st prototype but with a overstretching protection mechanism that prevents the spring from deformation above the 200 % extensional limit, and therefore, it limits the pressure produced. |
| Skin irritation | Long-time exposure to polyester fabric. | Wear the patient arm with a cotton sleeve and place it between the bracelet and skin. | Same as 1st prototype. |

**Table 8:** Potential risks for the patient and the actions adopted in first and second prototypes.

# CHAPTER 6:

# *Pressure and temperature testing*

In this chapter, the two prototypes presented before will be submitted to pressure and temperature testing using an experimental set-up to recreate the patient arm conditions. Ultimately, a final bracelet will be chosen according to the results obtained.

## 6.1. Experimental set-up

The desired goal for the experimental part was to work out a mechanism similar to arm conditions with the final aims of finding the most suitable prototype for performing the squeezing force, determining a power supply for the driving circuit and obtaining the pressure versus temperature responses to different duty cycles.

To perform the pressure measurement, first, a premature-infant-type manikin filled with air and made of a semi-rigid membrane was used. In the abdomen, it had an open valve to the atmosphere to inflate and deflate the manikin. When the valve was left open, a squeezing (i.e. volume change) would force it to retract back to its original volume. Therefore, assuming no air leakage due to bad sealing and the product P·V constant (i.e. ideal gas) it was attempted to place a pressure sensor and measure pressure changes over time. Nevertheless, it was observed that the pressure remained too low for slow squeezing forces applied. After studying the situation, it was concluded that whilst the semi-rigid membrane acted as an elastic material which opposed no force, due to the same principle, the air inside the manikin caused a volume change on the membrane and the pressure measured by the sensor did not reflect the true value.

The proposed solution was to use water instead of air because of its known incompressible properties. Therefore, it was considered to build a tailored arm using PVC cylinders of a known radius and length. In the center, a cut through was made equal to the bracelet width and length. The main reason was to stick a non-rigid elastic white tape in order to transmit the pressure to the fluid at the same time it ensured the cut was sealed and there were no pressure losses. The cylinder, was then hot glued to a manually operable valve to the SS19L pressure sensor interface by BIOPAC USA. The interface which was intentionally made for intra-arterial blood pressure measurement had a second connector which was sealed using a silicone tube and hot glue. The driving circuit was set to V input by the power supply and different PWM duty cycles were applied via a function generator by Agilent technologies USA. The input current was limited to 1.15 A, and measured using the power supply. The experiment setting is depicted in Figure 28 and Figure 29.

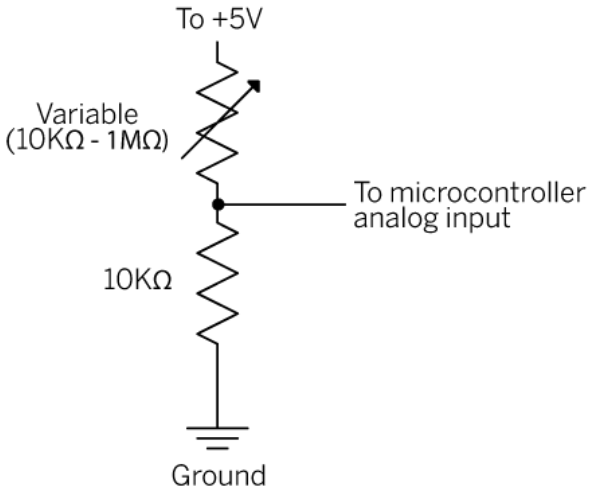


**Figure 27**: Voltage divider configuration for the temperature sensor.

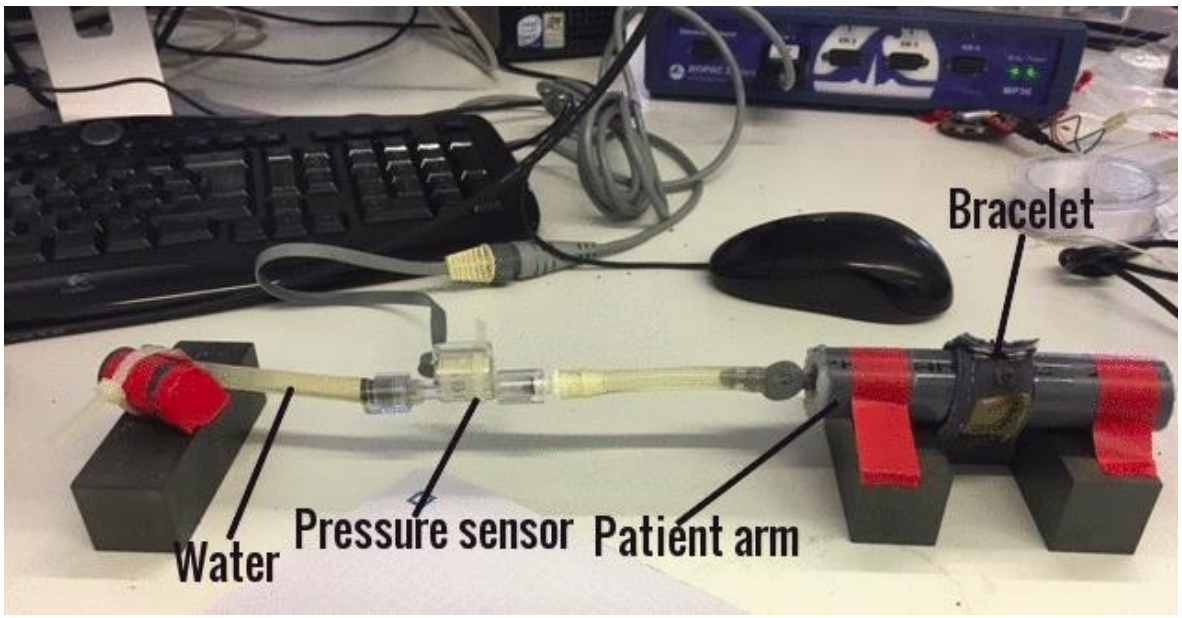


**Figure 28:** Experimental arm with water tubes and the bracelet wrapped around for pressure measurement.

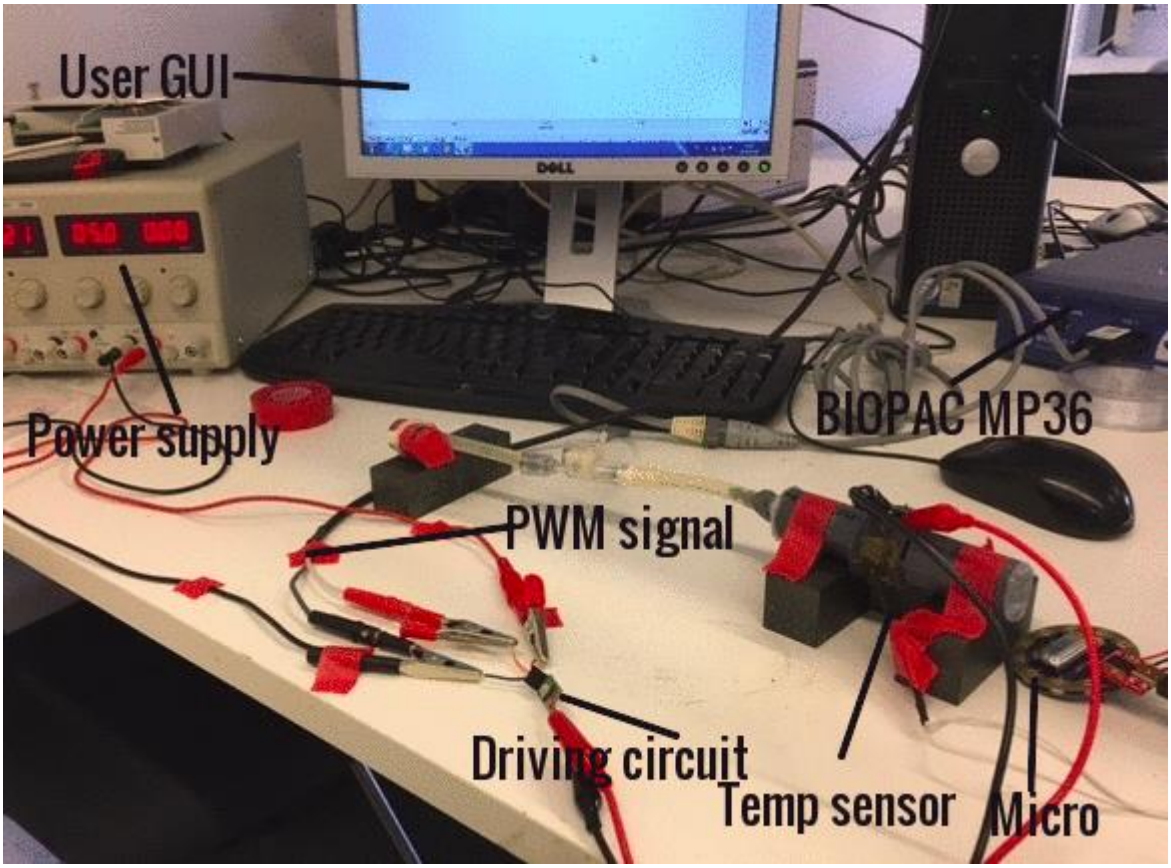


**Figure 29:** Full experimental set-up.

The sensor pressure SS19L was interfaced to the BIOPAC MP36 unit and preset to 'Pressure' configuration (Figure 28). Two low pass filters of 65.5 Hz and 38.5 Hz and a notch filter to 50 Hz were applied by software. The gain was set to 1000 and the values were calibrated to 0-200 mmHg range. Finally, the pressure was sampled to 20 samples/second.

For the temperature measurement, a NTC thermistor B57550 G550 8407 sensor by EPCOS Germany was connected to the arduino simblee in a voltage-divider configuration depicted in Figure 27, and sampled via the arduino 10-bit ADC. The datasheet provided the standardized R/T characteristic that were used to obtain temperature readings in ºC writing a script in MATLAB for real-time calculation. The analog readings were filtered with a moving average filter of 5 samples and sampled to 20 samples/second.

## 6.2. Results

There was a considerable interest in demonstrating that the second prototype had the best performance among the prototypes because it was more complex and accurately designed. However, the 4-spring configuration did not work as expected. The initial extensional force to extend the microsprings was too high for fitting it to the arm. Also, the pull lines detached from the microspring and fixing them was time-consuming and a complex task due to its dimensions (they had to be fixed under the microscope). Therefore, all the efforts were focused on working out the first prototype. In Table 9, Table 10 and the following figures, the most relevant information extracted from the experimental section is shown.

| **Test conditions: t(<=240s)** | $P_{max}$ **mmHg** | $P_{final}$ **mmHg** | **mmHg/s Up** | **mmHg/s Down** | **Power consumed at maximum pressure (W)** |
|---|---|---|---|---|---|
| **1) V++:** 5V **PWM:** 3.3V, 20% D.C | 58 | 23 | 2 | 0.4 | 1.17 |
| **2) V++:** 5V **PWM:** 3.3V, 30% D.C | 62 | 27 | 2.2 | 0.45 | 2.04 |
| **3) V++:** 5V **PWM:** 3.3V, 40% D.C | 70 | 27.5 | 3.6 | 0.5 | 2.75 |
| **4) V++:** 5V **PWM:** 3.3V, 50% D.C | 76 | 29.3 | 5 | 0.6 | 3 |
| **5) V++:** 5V **PWM:** 3.3V, % 60 D.C | 92 | 33.2 | 7 | 0.75 | 3.3 |
| **6) V++:** 5V **PWM:** 3.3V, 70% D.C | 108 | 40.4 | 8.5 | 1 | 3.5 |

**Table 9:** Pressure results.

| **Test conditions** $T_{initial} = 27.5ºC$ | $T_{max}(ºC)$ | $T_{transition}(ºC)$ | $T_{final}(ºC)$ | **ºC increase at 10 s** | **ºC drop at 10s** |
|---|---|---|---|---|---|
| **1) V++:** 5V **PWM:** 3.3V, 20% D.C | 40.7 | 30 | 27.5 | 3.7 | 3.5 |
| **2) V++:** 5V **PWM:** 3.3V, 30% D.C | 52.1 | 30 | 27.5 | 5.6 | 6.9 |
| **3) V++:** 5V **PWM:** 3.3V, 40% D.C | 53.9 | 30 | 27.7 | 6.7 | 7.65 |
| **4) V++:** 5V **PWM:** 3.3V, 50% D.C | 59.5 | 30 | 28.1 | 9.9 | 9.5 |
| **5) V++:** 5V **PWM:** 3.3V, % 60 D.C | 70 | 30 | 29 | 10 | 13 |
| **6) V++:** 5V **PWM:** 3.3V, 70% D.C | 71 | 30 | 29.7 | 10.2 | 12.55 |

**Table 10:** Temperature results.

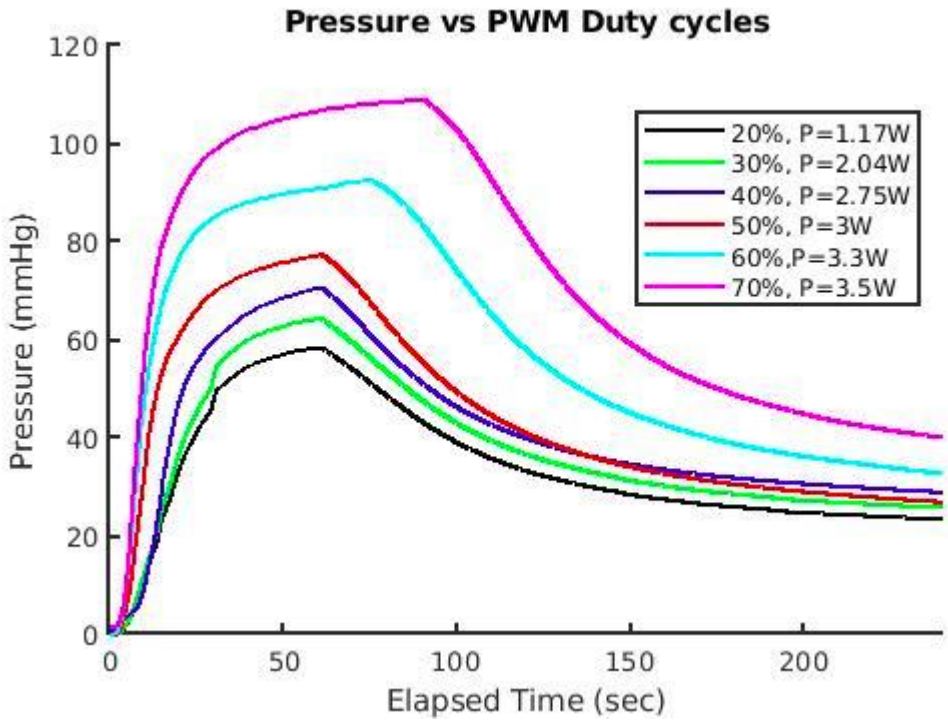


**Figure 30:** Pressure output vs. time for different PWM duty cycle outputs. The power consumed by the NiTi spring is presented in the legend. After smoothing the curves it can be observed that they follow the same

pattern: as soon as the transition temperature is achieved (30ºC) they quickly increase in pressure until their plateau. Then, when power is off (i.e. whether they reach the plateau or exceed the 100 mmHg limit) they follow a exponential decay to the final pressure. A maximum power of 3.5W is obtained in 70% duty cycle

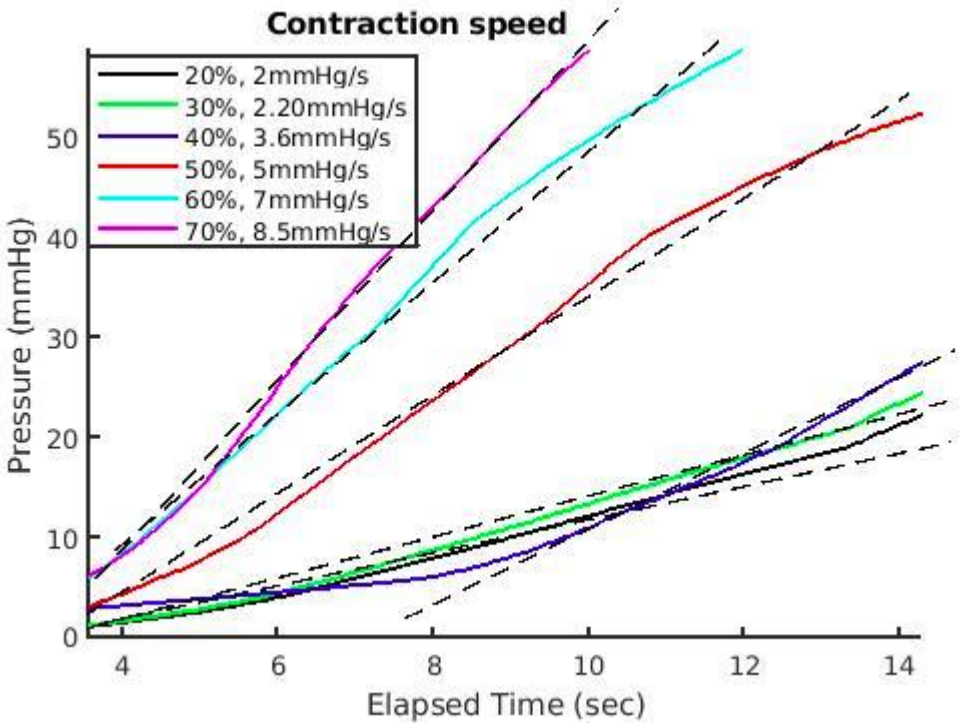


**Figure 31**: Pressure increasing speed according to the PWM duty cycle. The curves were least-squares fitted for the range shown and the corresponding slope was obtained.

.

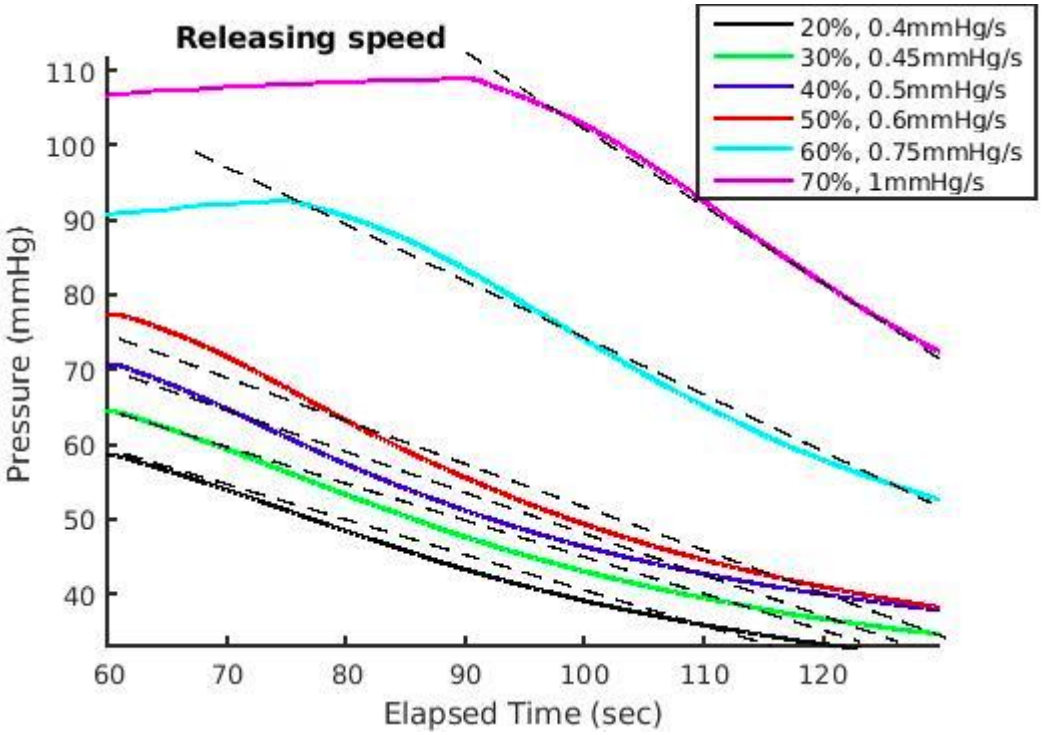


**Figure 32:** Pressure decreasing speed according to the PWM duty cycle. The slopes were obtained by least-squares fit to the curves.

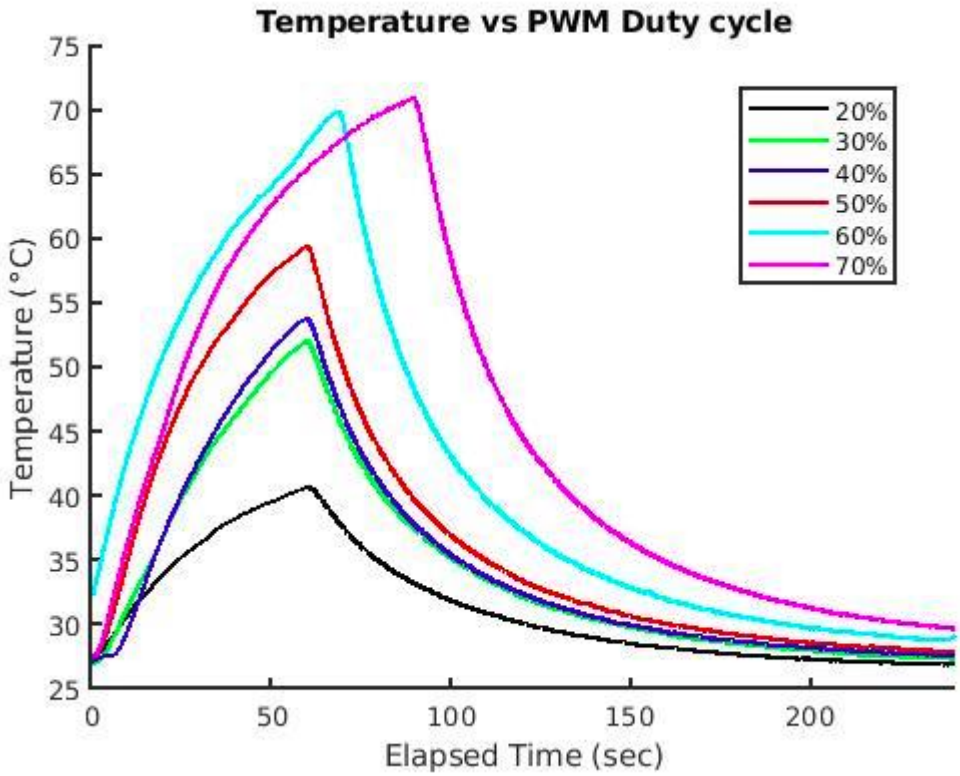


**Figure 33:** Temperature vs. time for different PWM duty cycle outputs. The curves were smoothed. It can be observed that by increasing the duty cycle the temperature arises much faster due to a longer exposure time to the current drawn by the driving circuit.

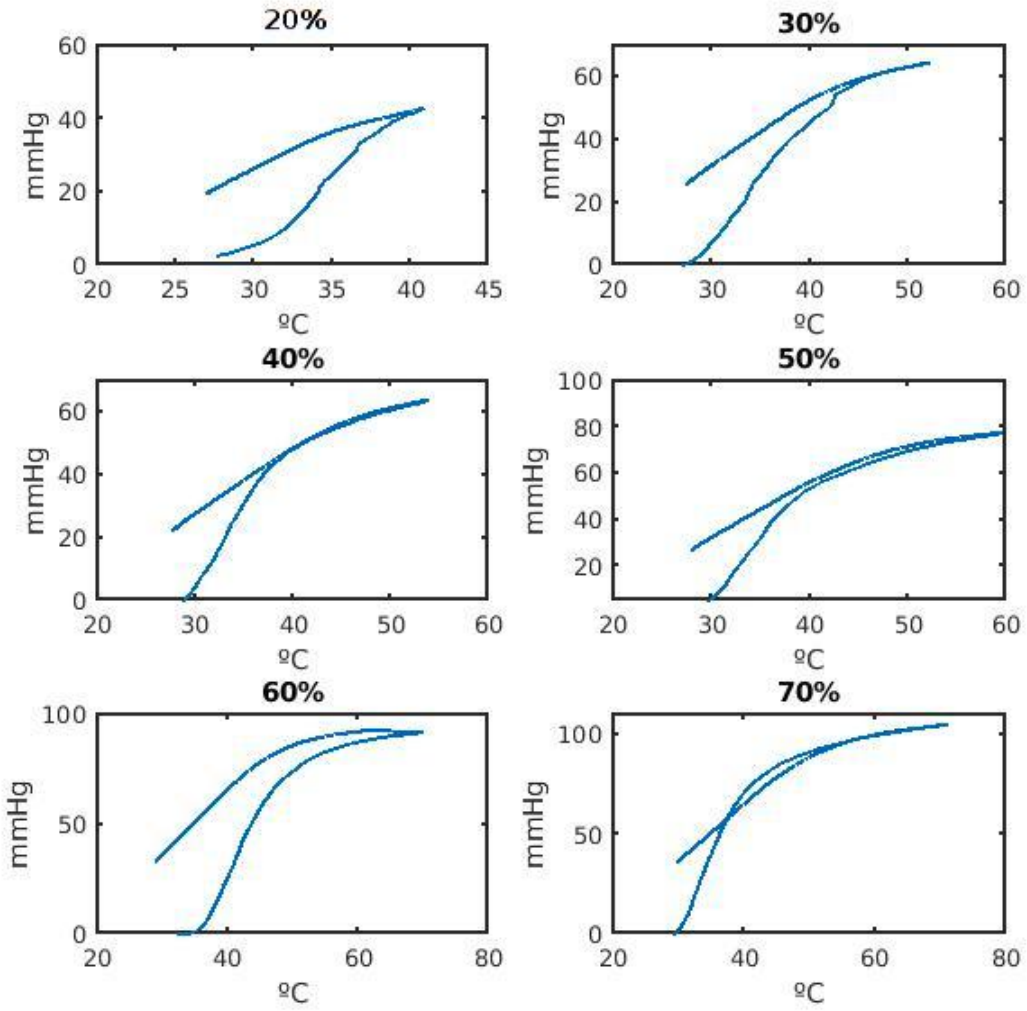


**Figure 34:** Loading and unloading cycles for different duty cycles. It can be observed the pressure hysteresis of the bracelet: the transformation begins when the pressure increases from 0 mmHg (when the transformation temperature is achieved) and is completed at maximum pressure (when the final transformation temperature is achieved). When the percentage of austenite fraction increases as the temperatures arises to the final temperature, the stiffness is increased due to a change in the crystalline structure of the alloy. This is documented in scientific literature as 'biased stiffness' [33] due to stress hysteresis of NiTi and is the reason why pressure follows a different path upon cooling, eventually resulting in a delay of the pressure and much more resistance to deformation.

## 6.3 Discussion

The bracelet from prototype 1, achieved pressure requirements and pressure range encompassed both target diastolic and systolic pressures. Pressure model succeed in predicting the maximum pressure and force model was of help to set up the strain limits. Also, thermal modelling set the basis for understanding current vs. temperature relation and exponential decay upon cooling which, with the existing gap in mind, theoretical model predicted quite well the spring cooling on air. Further, as expected, squeezing pressure depended mainly (excluding the spring parameters) of the voltage supplied to the driving circuit and increment of time supplied by PWM duty cycles.

One of the goals was to find out if the contraction speeds were in an acceptable range for performing blood pressure measurement when the pressure was increased. Eventually, this was mainly achieved by a power supply of 5 volts which provided enough voltage for having different contraction speeds. Also, a simple PWM duty cycle output directly controlled squeezing pressure. In the case when the diastolic and systolic range would be achieved (say $\pm$15mmHg of assumed pressure values in literature) the system could ultimately slow down the increasing speed in order to let the measurement sensors acquire more samples from that particular region, thus improving measurement accuracy.

However, the system had its drawbacks. Firstly, thanks to loading and unloading the bracelet, it was observed the pressure hysteresis effects at low pressure and low temperature values. When the spring was unloaded at its stress plateau, the stiffness increased and it was more resilient to deformation. Therefore, after the pressure exponentially decayed, the final value was generally 20 mmHg above initial pressure. This had to be addressed in the case a continuous and automatic blood pressure measurement was desired, otherwise, the bracelet would had to be removed from the baby's arm at each measurement and the spring stretched manually.

Although the scope of this project aimed at providing a system that measured blood pressure regardless of its continuous trend, it was considered that it might be of considerable interest to propose a solution that may guide others to tackle this problem.

Figure 35 shows the proposed solution. It was based on a two-way motion biasing springs made of stainless steel. One bias spring was placed at each end of the NiTi spring and sewed to the bracelet. Upon unloading cycle, NiTi spring would compress to its original length but the bias spring stored elastic energy, would force it to reduce its deflection by stretching it back to its detwinned martensite configuration (i.e. 200% strain). With this solution, it was intended to tackle another issue regarding the pressure distribution. When the spring was placed lengthwise, the force would be applied to the spring's contact area. Then, the foam function was to evenly distribute the result pressure along the width. However, in practice, it created a "U" shape and wasn't able to properly

absorb and distribute pressure. That's the reason a zigzag configuration depicted in Figure 35 was considered.

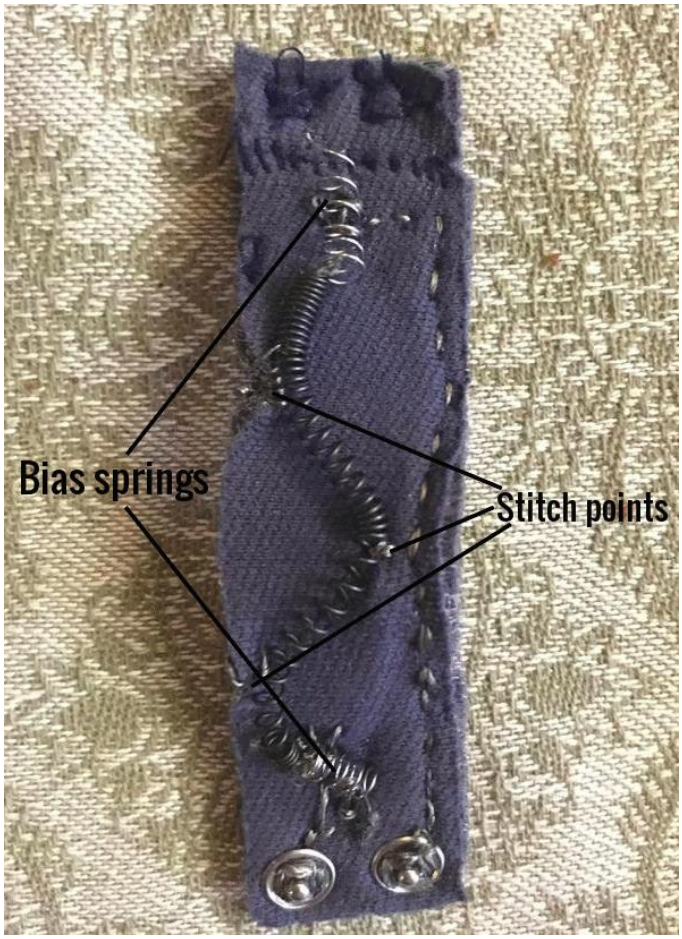


**Figure 35:** Proposed design to overcome the pressure hysteresis. In addition to the bias springs, a zigzag configuration was adopted to qualitatively assess a better pressure distribution along the bracelet width.

Although the bias springs worked as expected, the pressure reduction was virtually unperceivable. Also, the force exerted by the spring had to be compensated and consumed more power. On the other hand, the zigzag stitching did not resist the compression and the foam due to its elastic properties failed to hold the spring. Further research is required to understand and design the biasing spring mechanism. Also a pressure mapping test would help to design a mechanism for evenly distributing pressure to meet AHA recommendation.

Finally, spring's temperature peaked at 70ºC when the maximum duty cycle was provided. This reminded the importance of thermally insulating the spring and eventually, a 5 mm semi-rigid silicon tube covered the spring area. Also, the driving circuit, despite its copper heat sink, ended up heating up too much for not taking protection measures. Hence, it was covered the whole surface

with 4 Kapton 0.1 mm tape layers. Final design with aforementioned modifications is depicted in Figure 36.

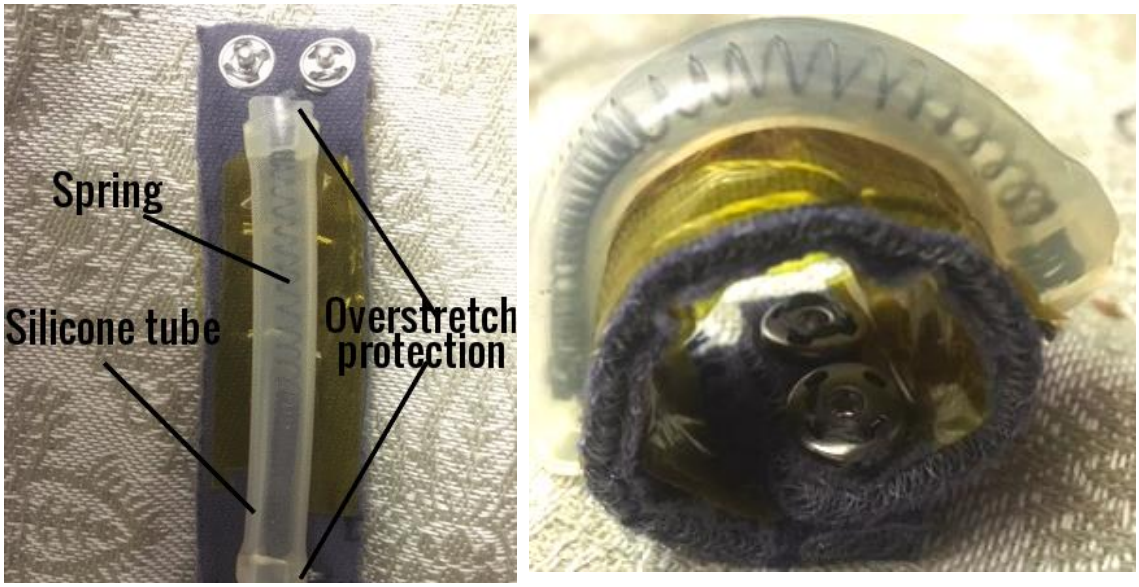


**Figure 36:** Final bracelet prototype stretched (left) and wrapped (right). Modifications regarding thermal insulation were adopted and inspired by the second prototype.

# Chapter 7:

# *Hardware*

In this chapter the electronics required for controlling the bracelet and performing the blood pressure measurement will be explained. Finally, the whole system will be integrated in a neonatal jacket.

## 7.1. Schematic

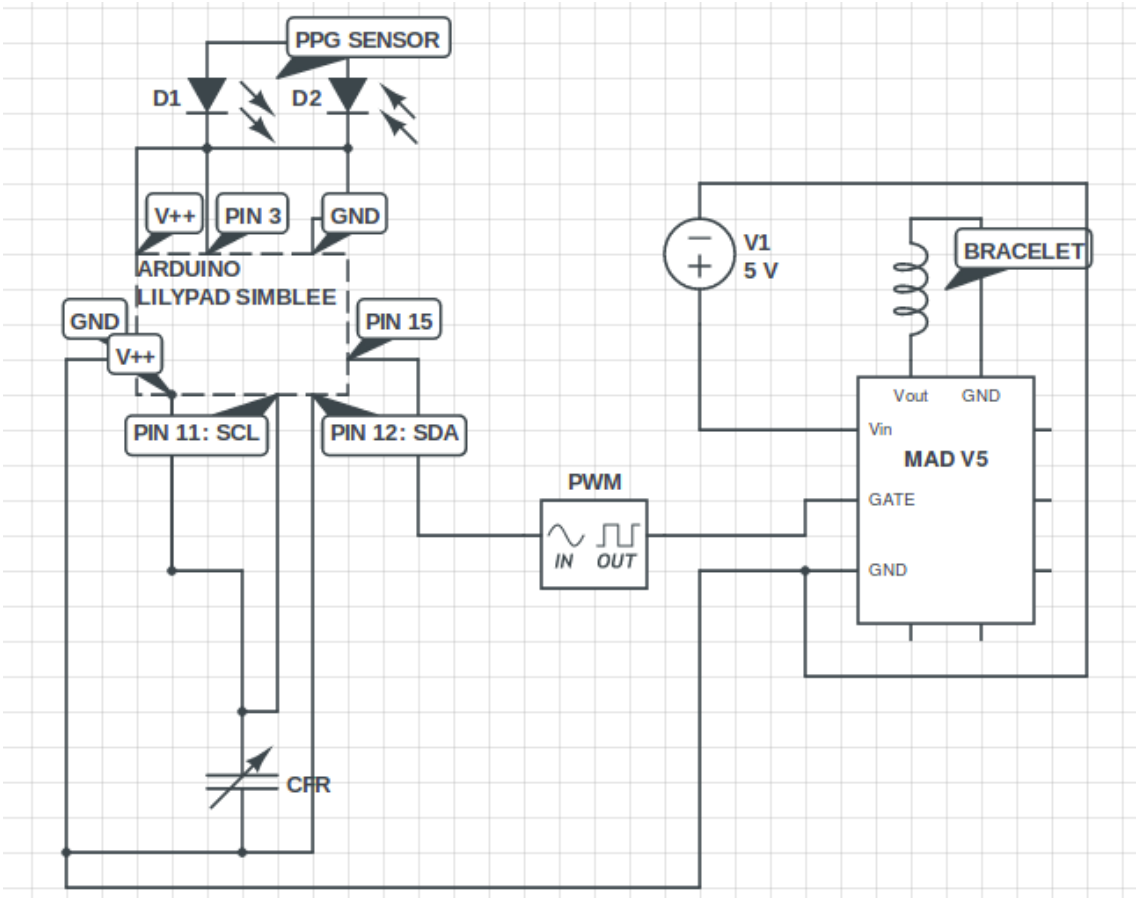


**Figure 37:** Schematic of the whole blood pressure system and their connections. The main board is an Arduino Lilypad Simblee that has five main functions: **1**- Send programmed PWM outputs to control the bracelet. **2**- Acquire and sample PPG sensor data. **3**- Acquire through I2C and sample CFR sensor data. **4**- Compute BP (Blood Pressure) and BPM (Beats per Minute) via a measurement algorithm. **5**- Send the data via BLE to a mobile user interface. The 5V battery connected to the MAD v5 circuit was determined in the experimental section. Pressure measurements are made thanks to CFR and blood volume oscillations are determined thanks to the pulse sensor.

## 7.2. Control unit: Lilypad Simblee

Lilypad is a family of Arduino-based microcontrollers boards that were conceived to be easily integrated in e-textile projects. It comes in different formats and characteristics: the Lilypad Simplesnap, Lilypad Simple board, Lilypad Simblee, etc. All three are sewable to fabrics and washable when the power supply is removed. It this project, the whole interface was built using the lilypad simblee because it works on BLE (Bluetooth Low Energy) and among all the boards is the smallest and the lightest. BLE provides great range medical applications and is relatively easy to use. BLE can sync and communicate with other BLE hosts like smartphones.

SIMBLEE chip was introduced in 2015 by RF Digital co It is a high performance, professional grade Bluetooth 4.0 transceiver with built in 32-bit ARM Cortex M0 processor. The processor can be programmed via Arduino IDE using 4 Simblee API's: Simblee BLE, SimbleeCOM, SimbleeForMobile and SimbleeCloud. It is often referred as IoT4EE (Internet of Things for Everyone and Everything) and it speeds up product development as it can directly upload GUI description code to cell phone working on OSX or Android using the Simblee application. Its built-in AES encryption engine for bi-directional communication, ensures data is securely managed a key aspect in medical applications.

The board has 4 cm diameter thin PCB with a JPE 2 mm pin for connecting a Lithium Polymer Battery with a built-in rechargeable and protection circuit. Also, each of the seven GPIO pins is a fabric wiring point sewable using conductive thread like stainless steel fibers ( R= 92$\Omega/m$). All the pins are ESD protected and it has the ability of redirect GPIO functionality around. This means that I2C, SPI, UART and analog/digital I/O can be switched to each of the 7 pins. It also includes a built-in temperature sensor, a LED, and of course a Bluetooth antenna. Tech specs including: digital I/O pins, operating voltage, among others are included in Table 11.

| | |
|---|---|
| **Processor** | ARM Cortex M0 32-bit |
| **Input Voltage** | 1.8-3.6V |
| **GPIO pins with redirect functionality** | 7 |
| **ADC** | 6 |
| **PWM** | 4 |
| **SPI** | 2 |
| **I2C** | 2 |
| **UART** | 1 |
| **ULP (Ultra Low Power sleep mode)** | 600nA |
| **DC Max. Current per I/O pin** | 40mA |
| **Flash Memory** | 128 KB ( 2 KB used by bootloader) |
| **SRAM** | 24KB |
| **Clock Speeds** | Onboard 16MHz and 3KHz |

**Table 11:** Lilypad Simblee BLE Board specifications [39].

## 7.3. Capacitive Force Sensor

In this section it was considered to perform the pressure measurement using Resistive Force Sensor (FSR) or Capacitive Force Sensor (CFS). The motivation to choose the first option was the price and availability in the local stores. After some testing, it was disregarded FSR due to: its low accuracy, low repeatability, high drift over days and the configuration were a source of problems: the voltage-divider configuration added the requirement of sewing a resistance into the textile which jeopardized the patient comfort and security. Moreover, FSR are subject to DC noise which introduces an amount of undesirable noise to the signal. FSR are considered to have low accuracy and to drift 0.75 mmHg per day so it impossibilities a long term monitoring and constant calibration is required [40]**.** For all those reasons, CFS was the only viable option.

CFS is a capacitive membrane of two electric conductors separated by a dielectric at a specific distance. When one of the surfaces is pressed it reduces the dielectric distance and as result, its differentiation of capacity produces an electric signal. CFS provides better repeatability, accuracy and overall performance than FSR that are based on the piezoelectric principle. CFS schematic is depicted at Figure 38.

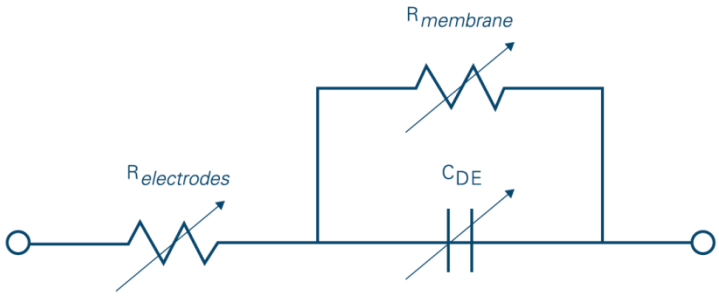


**Figure 38:** Equivalent circuit for dielectric elastomer sensor. $R_{membrane}$ and $R_{electrodes}$ are two resistances used to estimate the sensor capacitance as explained in [41].

Regarding this project application, it was found a commercial CFS that satisfied the following requirements:

- Repeatability error: < 1%.
- Low hysteresis.
- Linear response.
- <20mm sensing area.
- Low drift.
- High sensitivity.
- I2C circuit.
- Pressure range calibrated: 0-100 mmHg.

Finally CS15-4.5N from SingleTact was elected. With the calibrated version, a linear response for a force scale of < 4.5 N was obtained. It comes also with a data acquisition unit (DAQ) and I2C output to be fed into the microcontroller. I2C required pull up resistors which were set by the 10kΩ input resistors in the arduino board.

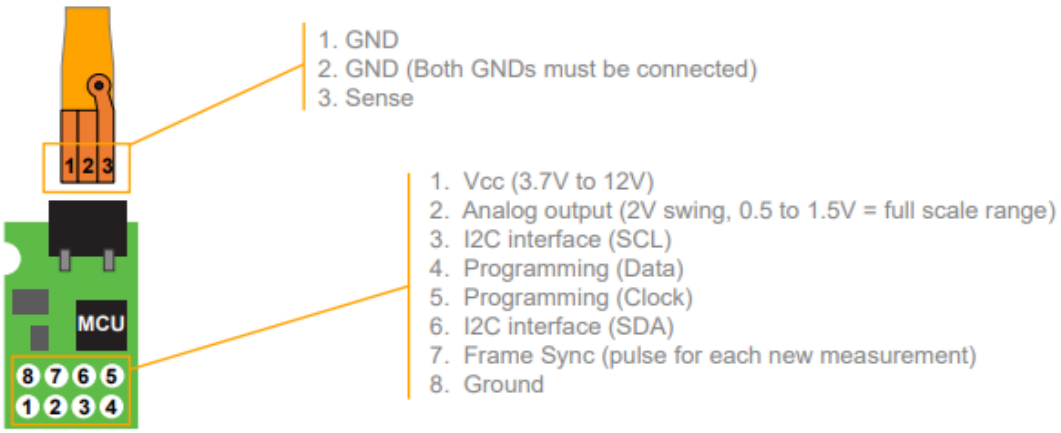


**Figure 39:** I2C circuit specs and diagram [42].

The electronic specifications of the integrated circuit are presented in Table 12.

| | |
|---|---|
| **Update rate** | >100Hz |
| **Analog Out** | 0.5-1.5V |
| **Digital Interface** | I2C (100kHz), 10-bit resolution |
| **Supply** | 3.7-12V |
| **IO Voltage** | 3.3V |
| **Weight** | 0.23g |
| **RoHs** | Compliant |
| **Sensing area** | 15mm diameter |
| **Operating temperature** | [-40ºC, 85ºC] |
| **Pressure resolution** | 0.1mmHg |
| **Response Time** | <1ms |

**Table 12:** Electronic specifications of CFR I2C [42].

## 7.4. MAD v5 driving circuit

To control the current that flows to the NiTi springs it was used an Arduino PWM pin together with a mosfet switch board. As seen in the micro specs, PWM pin current is just 40 mA and is not enough for changing the spring to its austenite phase and produce the desired force. Therefore, a current amplification mechanism was necessary. First, it was tested the spring using a TIP120 NPN transistor

in an emitter follower configuration. The transistor succeeded in providing up to 0.5 A to the spring but often resulted in overheating of the spring which eventually burned the components nearby. Also, TIP120 package did not have heat sinking so it was getting too hot. That is why it was necessary to look for a mosfet analog driver with SMD in a PCB format.

MAD v5 is a MOSFET switch from Miga Motor Company (U.S) that switches up to 30 V and 5 A. It can be switched by external control through PWM signals to a gate pin that connects when "HIGH" and disconnects the circuit when "LOW". It can also be switched by a push-button placed on the board. What makes it attractive is its small size (30x10mm) and that it has an overheating protection circuit to the actuator. This is achieved thanks to an end switch pin that gets raised "HIGH" to the input voltage on normal conditions and when it gets shorted to ground by a limit end switch contact to the spring, it cuts off the MOSFET and therefore, it prevents the spring from overheating.

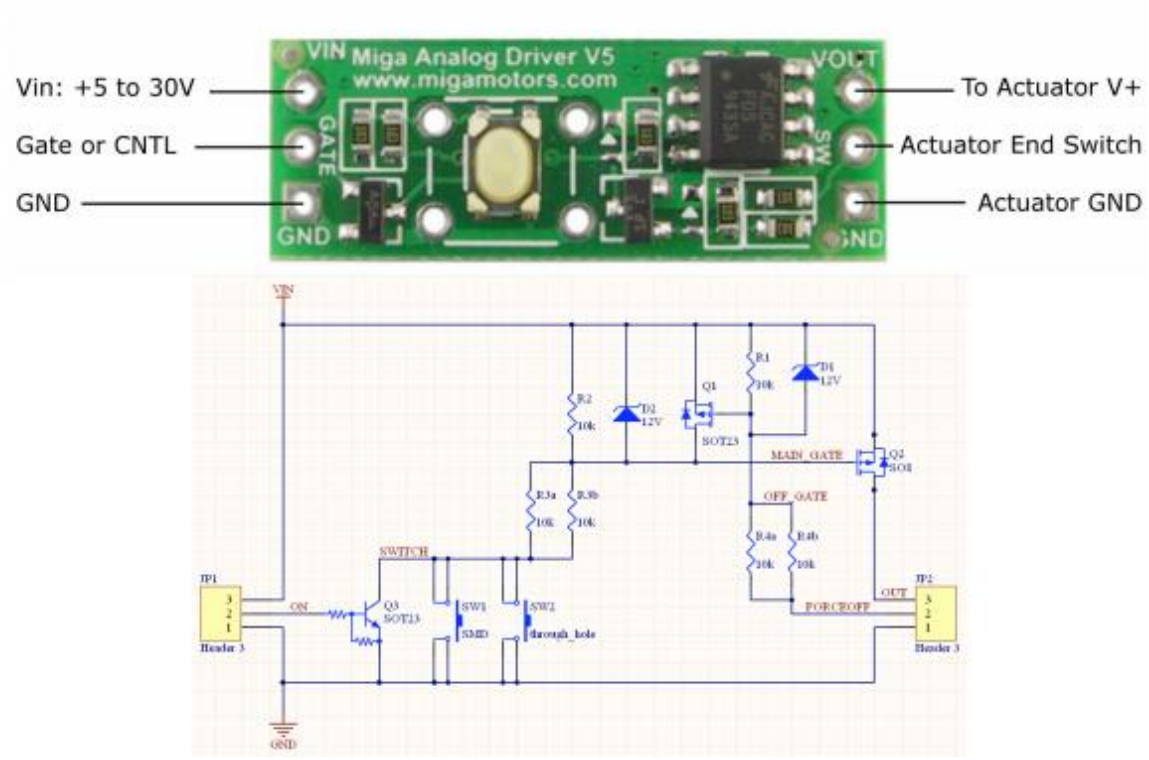


**Figure 40: Top:** Physical MAD v5 board with operational pins. It can be seen also the push-button of yellow appearance. **Below:** Circuit diagram of the board [43] **.**

## 7.5. Photoplethysmography Pulse sensor

The main reason to use pulse sensor technology was to obtain a clear differentiated blood volume signal to assess blood volume amplitude changes due to the application of pressure. However, signal amplitude is also dependent of many factors which sometimes may difficult its reliable

detection. Those are the input current to the LED which determines the SNR (Signal to Noise Ratio); skin tone, melanin (a natural pigment on skin) absorbs green light, therefore skins with a higher presence of melanin will require signal amplification; pressure applied on the sensor, among others. Hence, it was decided to obtain an integrated pulse sensor device which could be operated using Arduino and solved most of these issues.

Pulse sensor amped device (Figure 41) is a non-medical device used for measuring heart rate using PPG principles. It combines an optical heart rate sensor and provides signal amplification and noise-filtration circuitry. Also the PPG signal is normalized at voltage midpoint (i.e. V/2). The light wavelength is in the range of 470 nm (i.e. green) making it unable to measure deeper physiological parameters like SpO2 but is less affected by noise floor of ambient light [44]. The input current is optimized to maximize signal to noise ratio and the pressure applied is kept constant using a Velcro strap.


**Figure 41:** Pulse sensor amped device with 16mm diameter covered with vinyl stickers; front side (left image) and backside (right image) [45].

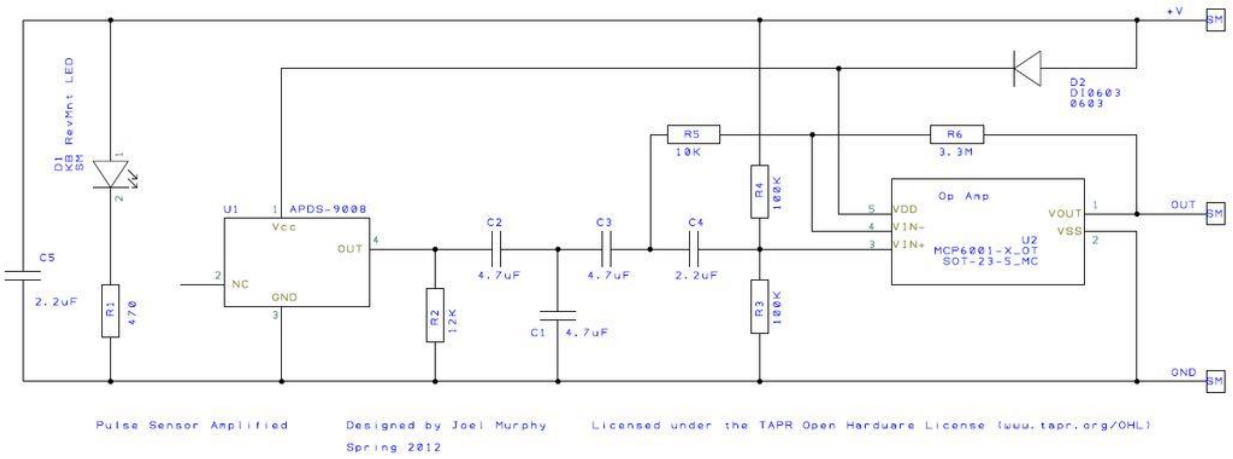


**Figure 42:** Pulse sensor integrated circuitry[46].

## 7.7. Textile integration

The whole blood pressure system with the aforementioned parts were integrated into a wearable neonatal jacket. It was employed stainless steel thread instead of copper wire and a novel insulated copper wire embedded in an elastic band (Figure 43) Also, the jacket was made of cotton fiber in the skin contact area in combination with polyester fibers to add strength on the surface. Further, a child-friendly design was given and a nice elephant was broidered. System is depicted in Figure 44 and Figure 45.

**Figure 43:** Elastic band with copper wire embedded.

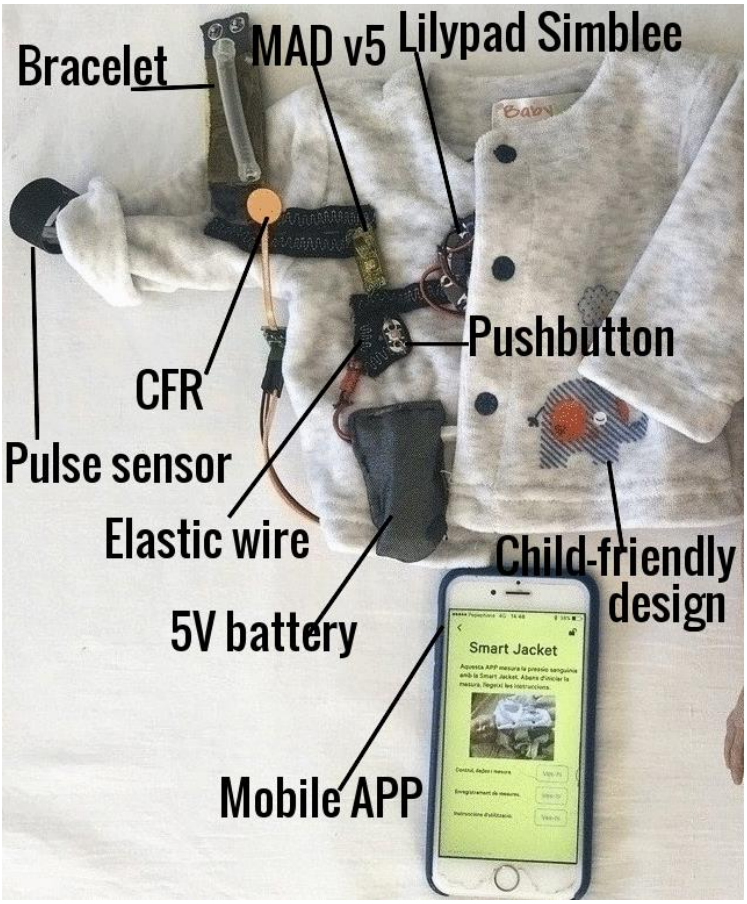


**Figure 44:** Smart jacked and its main components.

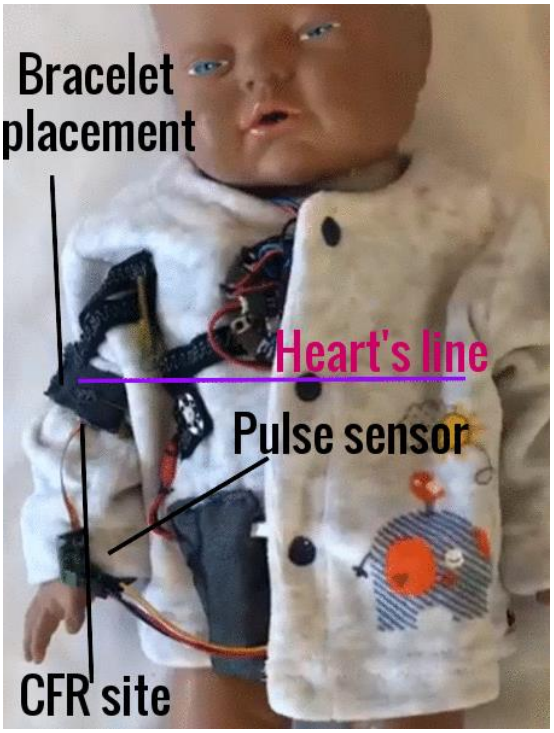


**Figure 45:** A premature manikin wearing the smart jacket. The bracelet must be placed at the heart's line for avoiding the hydrostatic pressure effect. Also, the CFR is placed between the bracelet and the jacket's sleeve and the pulse sensor wrapped at the wrist.

# Chapter 8:

# *Software*

In this last chapter, the blood pressure measurement algorithm will be explained step by step and finally, a mobile user interface powered using BLE will be described.

## 8.1. Blood pressure measurement

Among the blood pressure measurements presented in chapter 4, it was desired to make a semi-occlusive measurement method using the NiTi bracelet as actuator. However, the measurement had to be sensed somehow. At first, there was an attempt to employ Korotkoff sounds because it was relatively easy to integrate a microphone next to the force sensor and place it just below the bracelet. Nonetheless, it must be said that this solution had the problem of having to add a hardware amplification and filtration stages. While this might have been a time-consuming task for the textile integration, it was also found in the literature a study disregarding Korotkoff sounds in new-borns below 1 month old because it was not reliable enough [47]. Therefore, the next alternative consisted in making the measurement with one single sensor, the force sensor. The idea was to extract pulse oscillations from the sensor signal and its magnitude to calculate blood pressure. Although this kind of measurement is barely found in the scientific literature, it was concluded that the sensor sensitivity was not high enough and, further, the movement artefacts and added noise made it difficult to extract the desired features.

The remaining option was to add a second sensor to look up for the blood volume oscillations. This was achieved with the pulse sensor mentioned before. PPG captures changes in external pressure applied to the arm by blood perfusion. When a range of external compressing pressures are applied to the brachial artery, the PPG waveshape shows changes in amplitude and in the temporal pattern. When the external pressure arises, it causes a block to the arterial blood perfusion, affecting blood volume at the point of measurement and a shift of extra-cellular fluid in the tissue. This can be observed in the PPG's signal baseline that increases. At the same time, the PPG's signal amplitude will gradually increase to a maximum which is found to be related to MAP, and finally, it completely disappears at higher external compressions [48]. Likewise, it will gradually increase in the event of pressure release. This effect is shown in Figure 46.

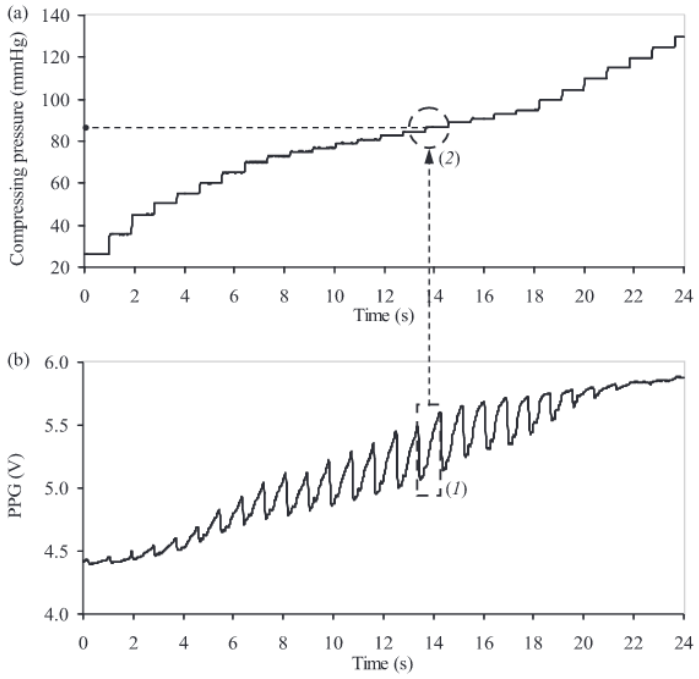


**Figure 46**: An example PPG signal (below) affected by local blood pressure variations at the measurement site (fingertip) due to external pressure applied on the brachial artery with an inflatable cuff (top) [48]**.**

Finally, a flowchart was designed to explain the procedure employed to measure blood pressure by the hand of the designed system (Figure 47). A set of user instructions for the smart jacket can be seen at Annex A.

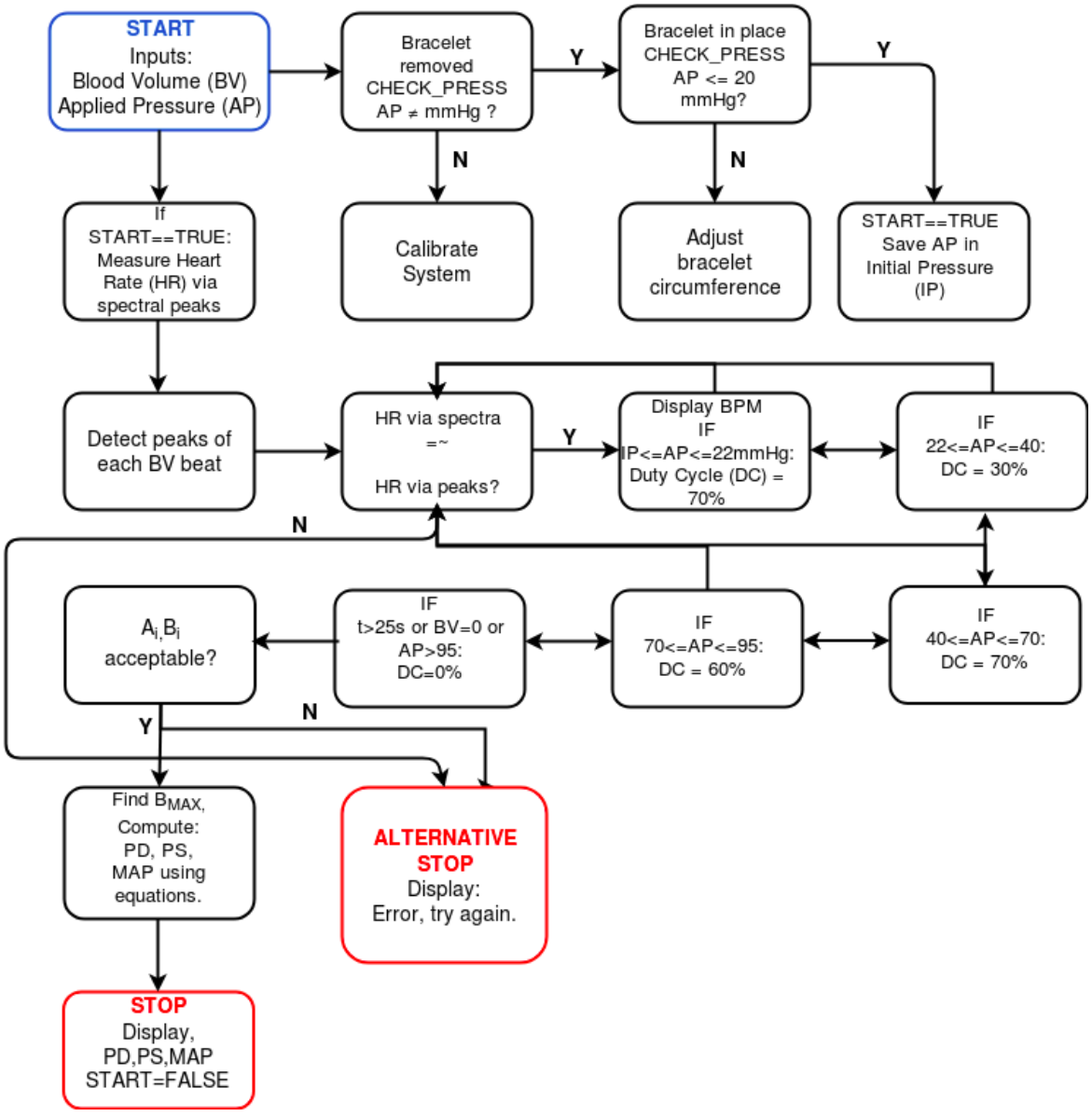


**Figure 47:** Flow chart of the proposed blood pressure measurement algorithm using the neonatal jacket.

The CHECK_PRESS function will be separated from the measurement algorithm in order to speed up the measurement time and provide the information apart at any time. Therefore, the user will be able to check for the pressure being within the limits at any time without the need for starting a new blood pressure measurement. However, note that to start the measurement the boolean variable START must have been set to TRUE by meeting the CHECK_PRESS requirements.

Firstly, the algorithm checks that the initial pressure on the bracelet is lower than 20 mmHg; a value determined empirically which is below the mean expected diastolic values in premature. Secondly, heart rate is calculated via the spectral peaks analysis. Blood volume signal is ADC (Analog to Digital Converted) and sampled to the 0.5-3 Hz range. The accuracy of FFT calculation is dependent of the

sampling duration. A sampling frequency ($F_S$) of 16 Hz was set and a total N samples of 256 were acquired in the duration of 16 s. Hence, the FFT accuracy was of:

$$\Delta f = \frac{F_s}{N_S \cdot F_S} = \frac{F_S}{t_s \cdot F_s} = \frac{1}{t_s} = \frac{1}{16} = 0.063\ Hz$$

**(Eq. 8.1)**

This means that the HR accuracy was the following:

$$HR_{Acc} = \frac{60 \cdot F_S \cdot \Delta_f}{N} = \frac{60 * 16 * 0.063}{256} = 0.24BPM$$

**(Eq. 8.2)**

An accuracy of 0.24 BPM from Eq. 8.2 is good enough for assessing if the measurement is free of movement artefacts and the blood waveforms are being well detected. During the whole PWM stage controlled by setting the bracelet at different duty cycles outputs, the waveform peaks are being detected and the heart rate calculated and displayed at real time and hence, compared with the heart rate obtained via spectral peaks. If at any time, the heart rates values are 10 % or more different from each other, the measurement will be stopped and a message of error will be displayed.

The duty cycles were set according to the increasing speeds determined experimentally in the previous Chapter 6. Whether the pressure is in the expected diastolic or systolic range, it slows down in order to get more samples for the further processing. The bracelet stops when blood volume signal is not detected (amplitude near 0), the pressure is above 95 mmHg (safety limit) or the elapsed time is more than 25 s. $A_i$, $B_i$ represent the amplitude blood volume values and the corresponding pressure values in a full squeezing cycle. If they fall out of the acceptable range, they will be filtered out and a message of error will be displayed. This will prevent from fake readings. The $A_i$, $B_i$ values are thereafter smoothed via a third-order polynomial fit and diastolic pressure (PD), systolic pressure (PS) and mean arterial pressure (MAP) computed and displayed according to the equations (Eq. 8.3, Eq. 8.4, Eq. 8.5) and acceptable parameters (Eq. 8.7, Eq. 8.8, Eq. 8.9).

Equations for BP measurement:

$$MAP = \frac{1}{2j}\sum_{i}^{2j} B_{\in \{A_{max-j}, A_{max+j}\}} \ [mmHg]$$

**(Eq. 8.3)**

where $\{A_{max-j}, A_{max+j}\}$ is the interval of $2j$ samples that follows the maximum amplitude value ($A_{max}$) in the PPG signal, and *j* is the integral value of $j = 10 * \frac{f_s}{BPM}$.

$$PS = \frac{1}{2p}\sum_{i}^{2p} B_{i \in \{A_{0-p}, A_{o+p}\}} \ [mmHg]$$

**(Eq. 8.4)**

where $\{A_{0-j}, A_{o+j}\}$ is the interval of *2p* samples that follows the zero amplitude value ($A_0$) in the PPG signal, and *p* is the integral value of $p = 10 * \frac{f_s}{BPM}$.

$$PD = \frac{1}{2}(3MAP - PS) \ [mmHg]$$

**(Eq. 8.5)**

Acceptable parameters:

$$0 < A_i < A_{MAX}$$

**(Eq. 8.6)**

$$A_{FINAL} \leq 0.5A_{MAX}$$

**(Eq. 8.7)**

$$A_{B=40} \leq 0.8A_{MAX}$$

**(Eq. 8.8)**

The acceptable parameters for computing systolic, diastolic and mean blood pressure were adapted from [49]**.** Also the equations Eq. 8.3, Eq. 8.4 and Eq. 8.5 represent a theoretical approach and do not have any validity unless its accuracy is compared to those obtained with a standard blood pressure method. In this work, it was not possible to test the prototype directly on a patient,

because it was not validated by the AEMPS (Agencia Española de Medicamentos y Productos Sanitarios) and by a local ethic committee for making measurements on humans. However, in a future implementation of a regulated system with the PS 93/42/EEC certification, the prototype could be used for direct measurements of blood volume signal changes to pressure applied, and hence, an empirical formula calculated. To mention some of the points from the current system that should be addressed and actions to get the necessary regulation:

- the components not manufactured but liable to the system by their action (i.e. pulse sensor, pressure sensor and Lilypad Simblee) must be independently assessed and decided whether they can exhibit (i.e. by quality, safety and usefulness ) the required performance of a medical device as stated in the 2001/83/EC directive.
- the thermal and electrical isolation measures adopted to guarantee the safety must go through an in-depth analysis to qualitatively verify that present no risk to the safety.
- the bracelet actuator must go through an in-depth analysis to verify there's no inherent risks arising from aging of materials used or loss of control mechanisms (e.g. by performing a stress test and life cycle test) and that the pressure is equally distributed.
- the system which aims to measure blood pressure must be able to demonstrate its accuracy and stability within its readings.
- the system also must include proper alarm systems (e.g. app notifications or external LED) to alert the person-in charge when the blood pressure readings indicate the danger of the patient's health.

## 8.2. IoT framework

A system architecture has been developed to test the blood pressure measurement sensors IoT (Internet of Things) functionality as illustrated in Figure 48. The architecture is fully compatible with the current system developed, so no hardware modifications needed to be made. The built-in bidirectional BLE (Bluetooth Low Energy) from the Simblee chip was exploited to create a mobile application working both on Android and iOS systems. The arduino libraries for Simblee, provided enough documentation from learning how to code the application and feature sensors information and control over the jacket to the user.

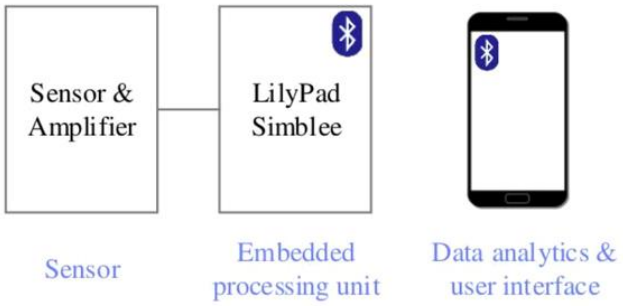


**Figure 48:** System architecture composed by the Smart Jacket sensors, the LilyPad Simblee BLE and a mobile application with data analytics and user interface.

To run the application, it is just required to install the Simblee Mobile App downloadable from the App Store or Play Store, and to interface the app with the jacket via BLE as a usual Bluetooth device. For security reasons, only 1 mobile device is able to connect to the jacket at the same time. When someone is already connected and using the application with the jacket on, it is impossible to connect to it by using a second mobile device. Also, to properly connect to the jacket, the mobile device must be within the maximum range of 10 meters. This prevents, that an unknown user, not explicitly belonging to the clinical staff, takes over the jacket. A full set of instructions is provided to the user (See Annex A).

The application is divided in three main screens. The control, data and measurement screen, a registration screen, and instructions screen (Figure 49). The control, data and measurement screen enables blood pressure measurement, provides information of the system's sensors when the bracelet is deactivated (CPU temperature, pressure and BPM), and systolic, diastolic and mean pressure values when the blood pressure is measured by activating the bracelet. All the data obtained, thus having personal information from the patient, is securely sent to the application using built-in AES encryption from the Simblee chip.

When a blood pressure measurement is successfully performed, the measurements are automatically registered in the "Registration screen" with timestamp and user information. Multiple measurements can be performed with multiple users (the jacket must be previously washed making special attention to remove the non-washable components, i.e. battery, and sensors) and in order to save them, the user can take a screenshot using his mobile device.

Finally, the application includes jacket utilization steps and instructions by clicking upon a permanent link, which the user is obliged to read and get acquaintance of them for a successful and secure use of the system.

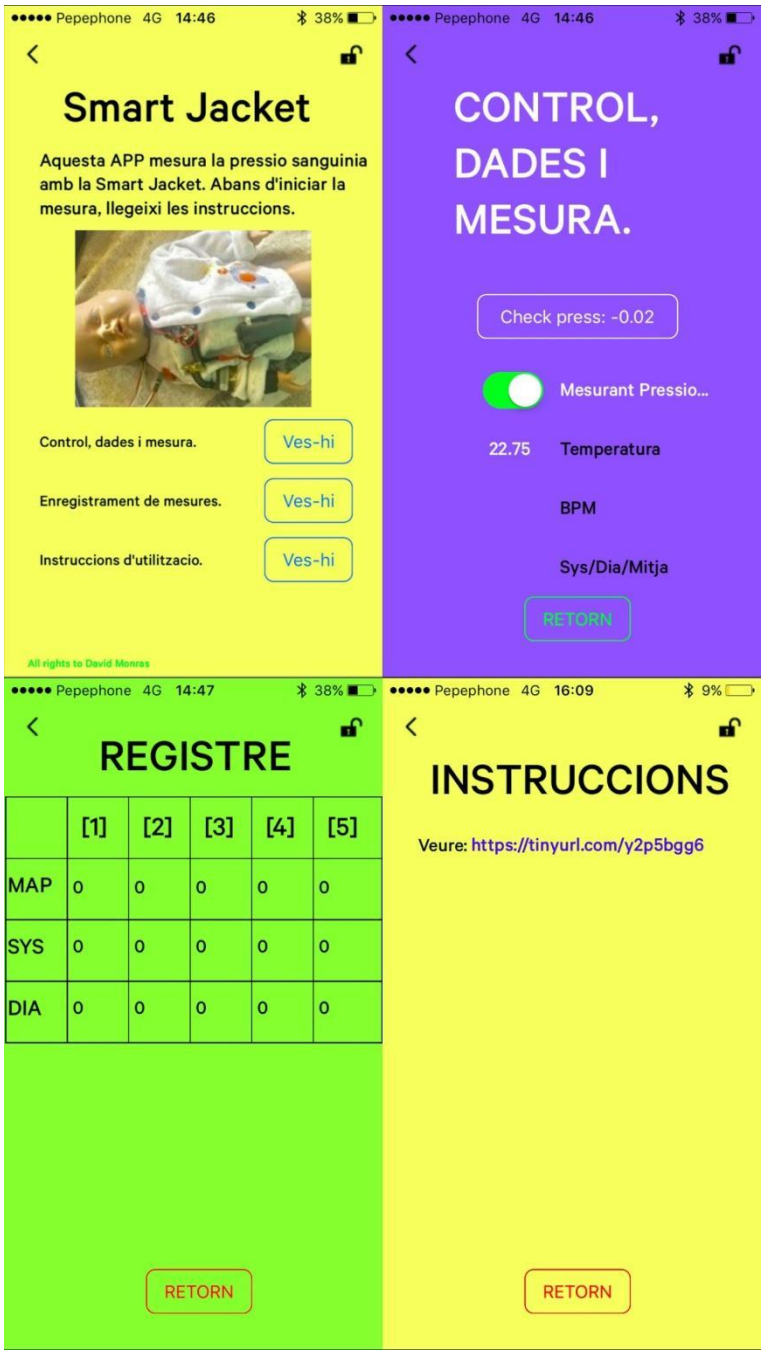


**Figure 49:** Mobile APP and its three screens. **Top-left:** Main screen. **Top-right:** Control screen. **Bottom-left:** Registration screen. **Bottom-right:** Instructions screen.

# Chapter 9:

## *Environmental Impact*

All the corresponding elements that constitute the prototype including: Lilypad Simblee board, optical sensor, pressure sensor, nitinol spring and the lithium batteries are compliant with RoHS 2011/65CE normative in their manufacture.

The material used during the testing (i.e. accessories, tools, electronic components…) of the prototype were mostly reused and taken from the tutor's electronic department laboratory. Also, the elastic cables were recycled from a previous project.

During the smart jacket use, the batteries are naturally consumed to power the electronic devices. The Lilypad Simblee board has automatic ultra-low power consumption when the Bluetooth is not strictly necessary, however, the remaining electronic devices do not. The batteries are rechargeable which considerably reduce the amount of waste.

The total energy consumed for the project is estimated to be of 33.15kWh. To see the full calculation refer to Annex C.

Finally, all the components can be individually separated and recycled at the end of their useful life.

# Conclusions

The novel smart jacket may be elected to perform blood pressure measurements in preterm infants in a near future if its application is validated for the measurement on human beings. Given that, a comparative study could be made and the benefits that in this project are pointed out finally proved. To support this assumption, it will list the deductions shown in this project.

The shape memory alloy bracelet is controllable at least during the contraction cycle, and therefore, a non-continuous blood pressure measurement is possible during the same. The spring responded to the variable duty cycles applied and reached its peak above the higher pressure and temperature value required for the measurement. Likewise, the transition temperature of 30ºC proved to be higher than the temperature at the incubators and therefore the smart jacket can be used while the baby is inside. However, the bracelet have to be removed at the end of each measurement because of the spring hysteresis which will require more research to finally reset it back to the original position, e.g. by using a bias-spring system, in the scenario of continuous measurement.

The blood pressure measurement using the smart jacket may be fully adapted to the needs of clinical use. The task for medical employers is more effortless by: firstly, integrating electronics directly to the smart jacket to the extent of “put it on to start measuring” and secondly, providing a functional mobile app working wirelessly for control, measure and registration of: systolic, diastolic, mean arterial pressure and beats-per-minute of the patient. Besides, the smart jacket can be easily washed if the batteries and sensors are previously removed, and hence, used for the measurement to other patients.

Smart jacket makes sure that the security to the patient and from data-transfer is guaranteed. The initially exposed parts to the patient were electrically insulated using kapton tape, sewing a double layer of thread and sewing an elastic and fully insulated layer of copper wire. The fabric includes natural cotton fiber to reduce the risk of the baby skin irritation. The spring tests, pointed out the necessity of thermal isolation to avoid damage for the high heating of the spring. A solution was adopted by covering it with a silicon tube. Also, to power the bracelet a mechanical push-button must be pressed, hence automatically stopping the compression when is released. Finally, the sending of personal information from the sensors to the mobile app is protected with AES encryption running on the board.

The mobile application enables the medical staff to measure and control the smart jacket at distance. At the moment, the application is powered using Bluetooth low energy which increases

the battery life compared to Wi-Fi boards. In the future, the distance could be increased to everywhere and web services like cloud storage available if the system is Wi-Fi compatible.

# Recommendations

Further research should be made to develop a pressure bracelet working with shape memory alloy springs that effectively gets back to its original length after one full compression cycle. In this project, a bias spring was proposed but the results were not successful. Also, a life-cycle testing of the spring is necessary to provide useful information on how many cycles for a given stress the spring can handle before it has to be replaced.

Further tests should be carried to map the pressure distribution of the bracelet in the jacket and eventually, to the patient arm. In this project, it was assumed that an even pressure distribution along the bracelet was possible by using a foam that explicitly was made for this purpose and following the AHA design recommendations for standard inflatable cuffs.

# Economic considerations

This chapter presents the economic considerations based on the expenses that results from the development of the prototype. The cost associated to the engineering hours is the highest outlay, followed by the list of materials needed to build the prototype. The software employed for coding was open-source so there was no cost associated. Table 13 shows the components total cost and Table 14 shows the activity costs. The total cost of the project is 21378.27 €.

| Component | Supplier | Cost |
|---|---|---|
| Kapton tape, baby fabric | Amazon | 38.71€ |
| Accessories, tools, arduino board | Sparkfun | 175€ |
| Pulse sensor | DFRobot | 52.91€ |
| Accessories for the 2nd prototype | Pecheur | 11.8€ |
| Capacitance force sensor | Singletact | 86.56€ |
| Nitinol springs | Kelloggs Research Lab | 180.4€ |
| Accessories | Onda Radio | 44€ |
| Accessories | Todoelectronica | 29.23€ |
| Accessories | Electan | 39.8€ |
| | | **TOTAL: 758.27€** |

**Table 13:** Expenses associated with the materials purchased to build the prototype.

| Activity | Price | Amount | Cost |
|---|---|---|---|
| Concept prototype design | 40€/h | 280 | 11200€ |
| Documentation | 40€/h | 20 | 800€ |
| Prototype testing | 100€/h | 30 | 3000€ |
| Software developing | 20€/h | 120 | 2400€ |
| Technical report | 40€/h | 50 | 2000€ |
| Shipping expenses | | | 220€ |
| Components | | | 758.27€ |
| | | | **TOTAL: 21378.27€** |

**Table 14:** Economic considerations for the project.

# References


[1] S. Schneegass and O. Amft, *Smart Textiles: Fundamentals, Design, and Interaction*. Springer, 2017.

[2] texperts, "By 2020: Smart Textiles Market Will Be Worth 4,722.81 Million USD | Welcome to Texperts." [Online]. Available: http://www.thetexperts.com/product-innovate/by-2020-smart-textiles-market-will-be-worth-4722-81-million-usd/. [Accessed: 21-May-2019].

[3] R. Paradiso, G. Loriga, and N. Taccini, "A wearable health care system based on knitted integrated sensors," *IEEE Trans. Inf. Technol. Biomed.*, vol. 9, no. 3, pp. 337–344, Sep. 2005.

[4] C.-T. Huang, C.-F. Tang, and C.-L. Shen, "A Wearable Textile for Monitoring Respiration, Using a Yarn-Based Sensor," *2006 10th IEEE International Symposium on Wearable Computers*. 2006.

[5] T. Linz, L. Gourmelon, and G. Langereis, "Contactless EMG sensors embroidered onto textile," *4th International Workshop on Wearable and Implantable Body Sensor Networks (BSN 2007)*. pp. 29–34.

[6] J. O'Donoghue and J. Herbert, "Data Management within mHealth Environments," *Journal of Data and Information Quality*, vol. 4, no. 1. pp. 1–20, 2012.

[7] A. Shafti, R. B. Ribas Manero, A. M. Borg, K. Althoefer, and M. J. Howard, "Designing embroidered electrodes for wearable surface electromyography," *2016 IEEE International Conference on Robotics and Automation (ICRA)*. 2016.

[8] S. Bouwstra, W. Chen, L. Feijs, and S. B. Oetomo, "Smart Jacket Design for Neonatal Monitoring with Wearable Sensors," *2009 Sixth International Workshop on Wearable and Implantable Body Sensor Networks*. 2009.

[9] M. Rothmaier, B. Selm, S. Spichtig, D. Haensse, and M. Wolf, "Photonic textiles for pulse oximetry," *Opt. Express*, vol. 16, no. 17, pp. 12973–12986, Aug. 2008.

[10] N. Luo *et al.*, "Textile-Enabled Highly Reproducible Flexible Pressure Sensors for Cardiovascular Monitoring," *Advanced Materials Technologies*, vol. 3, no. 1. p. 1700222, 2018.

[11] Y.-T. Zhang, C. C. Y. Poon, C.-H. Chan, M. W. W. Tsang, and K.-F. Wu, "A Health-Shirt using e-Textile Materials for the Continuous and Cuffless Monitoring of Arterial Blood Pressure," *2006 3rd IEEE/EMBS International Summer School on Medical Devices and Biosensors*. 2006.

[12] W. Chen, S. Dols, S. B. Oetomo, and L. Feijs, "Monitoring body temperature of newborn infants at neonatal intensive care units using wearable sensors," *Proceedings of the Fifth International Conference on Body Area Networks - BodyNets '10*. 2010.

[13] "NICU – suddenly inspired." [Online]. Available: https://suddenlyinspired.wordpress.com/tag/nicu/. [Accessed: 21-May-2019].

[14] Josep Maria Solà, R. M. (Electrotechnician), and O. Chételat, *Continuous Non-invasive Blood Pressure Estimation*. 2011.

[15] F. G.-M. Rodrigo, F. García-Muñoz Rodrigo, S. Rivero Rodríguez, A. Florido Rodríguez, F. G. Martín Cruz, and R. Díaz Pulido, "La ventilación ajustada neuralmente es eficaz en el destete y la extubación del recién nacido prematuro," *Anales de Pediatría*, vol. 82, no. 1. pp. e126–e130, 2015.

[16] J. M. Dionne, C. L. Abitbol, and J. T. Flynn, "Erratum to: Hypertension in infancy: diagnosis, management and outcome," *Pediatric Nephrology*, vol. 27, no. 1. pp. 159–160, 2012.

[17] A. L. Kent, S. Meskell, M. C. Falk, and B. Shadbolt, "Normative blood pressure data in non-ventilated premature neonates from 28–36 weeks gestation," *Pediatric Nephrology*, vol. 24, no. 1. pp. 141–146, 2009.

[18] N. van Helmond, T. B. Plante, and J. I. Joseph, "Blood Pressure Measurement Validation Off the Cuff? Comment on 'A New Cuffless Device for Measuring Blood Pressure: A Real-Life Validation Study,'" *J. Med. Internet Res.*, vol. 20, no. 10, p. e10089, Oct. 2018.
[19] H. Kaur, S. Agrawal, and S. Singh, "Fast and accurate method for continuous BP measurement," vol. 8, no. 2, pp. 13791–13802, Jun. 2016.
[20] M. Ramsey, "Blood pressure monitoring: Automated oscillometric devices," *Journal of Clinical Monitoring*, vol. 7, no. 1. pp. 56–67, 1991.
[21] HauteSingleMama and V. my C. Profile, "Fight For Preemies." [Online]. Available: http://hautesinglemama.blogspot.com/2010/11/fight-for-preemies.html. [Accessed: 21-May-2019].
[22] C.-H. Kuo, C.-J. Wu, H.-C. Chou, G.-T. Chen, and Y.-C. Kuo, "Development of a Blood Pressure Measurement Instrument with Active Cuff Pressure Control Schemes," *J. Healthc. Eng.*, vol. 2017, p. 9128745, Oct. 2017.
[23] J. Solà, M. Proença, F. Braun, N. Pierrel, and P. Schoettker, "Continuous non-invasive monitoring of blood pressure in the operating room: A cuffless optical technology at the fingertip," in *BMT2016 - "Dreiländertagung" Swiss, Austrian and German Societies of Biomedical Engineering*, 2016, vol. 2.
[24] A. I. O. Zaid and S. M. A. Al-Qawabah, "Effect of Cutting Parameters on the Quality of the Machined Surface of Cu-Zn-Al Shape Memory Alloy, SMA," *Advanced Materials Research*, vol. 1105. pp. 93–98, 2015.
[25] M. Fouda, M. Tawfik, and G. Elbayoumi, "Calibration of The Hysteresis Loop of SMA Wires Heated by Electric Current," in *15th International Conference on Applied Mechanics and Mechanical Engineering*, 2012.
[26] Dynalloy, "DYNALLOY, Inc. | Shape Memory Alloy Actuator Wire Manufacturer." [Online]. Available: http://www.dynalloy.com/. [Accessed: 21-May-2019].
[27] S. J. Yates and A. L. Kalamkarov, "Experimental Study of Helical Shape Memory Alloy Actuators: Effects of Design and Operating Parameters on Thermal Transients and Stroke," *Metals - Open Access Metallurgy Journal*, vol. 3, no. 1, pp. 123–149, Feb. 2013.
[28] Engrasp, Inc, "Engrasp." [Online]. Available: http://www.mahonkin.com/~milktree/hawk/springs-from-that-place/spring_help.html. [Accessed: 21-May-2019].
[29] B. Holschuh, E. W. Obropta, and D. Newman, "Low Spring Index NiTi Coil Actuators for Use in Active Compression Garments," *IEEE/ASME Trans. Mechatron.*, vol. 20, no. 3, pp. 1264–1277, Jun. 2015.
[30] B. Holschuh, E. Obropta, and D. Newman, "Shape Memory Alloy (SMA) Coil Actuators for Use in Controllable Mechanical Counter-Pressure (MCP) Space Suits," Feb. 2013.
[31] V. Kumar, R. Tikkas, S. Ramteke, and J. Shrivastava, "Assessment of gestational age using anthropometric parameters: an observational study in India," *Pediatric Review: International Journal of Pediatric Research*, vol. 4, no. 11, Nov. 2017.
[32] E. al Veiga EV, "Blood pressure measurement: arm circumference and cuff size availability. - PubMed - NCBI." [Online]. Available: https://www.ncbi.nlm.nih.gov/pubmed/19820850. [Accessed: 21-May-2019].
[33] H. Talebi, H. Golestanian, M. R. Zakerzadeh, and H. Homaei, "Thermoelectric Heat Transfer Modeling of Shape Memory Alloy Actuators," in *The 22st Annual International Conference on Mechanical Engineering-ISME2014*, 2014.
[34] "Technical Textiles & Knitted Fabrics - Baltex." [Online]. Available: https://www.baltex.co.uk/. [Accessed: 21-May-2019].
[35] "Technical Textiles & Knitted Fabrics - Baltex." [Online]. Available:

https://www.baltex.co.uk/. [Accessed: 21-May-2019].
[36] S. Naqvi, M. D. Husain, P. Potluri, P. Mandal, and P. Lewis, “Pressure distribution under different types of blood pressure measurement cuffs,” *J. Ind. Text.*, vol. 47, no. 1, Mar. 2016.
[37] R. Vaishya, A. K. Agarwal, M. Tiwari, A. Vaish, V. Vijay, and Y. Nigam, “Medical textiles in orthopedics: An overview,” *Journal of Clinical Orthopaedics and Trauma*, vol. 9. pp. S26–S33, 2018.
[38] A. Gupta, A. A. R. Irudayaraj, and R. Balakrishnan, “HapticClench,” *Proceedings of the 30th Annual ACM Symposium on User Interface Software and Technology - UIST ’17*. 2017.
[39] “Simblee.” [Online]. Available: www.simblee.com. [Accessed: 21-May-2019].
[40] R. Puers, “Capacitive sensors: When and how to use them,” *Sensors and Actuators A: Physical*, vol. 37–38. pp. 93–105, 1993.
[41] stretchsense, “Capacitive vs. Resistive Strain/Stretch Measurement - StretchSense,” *StretchSense*, 03-Feb-2017. [Online]. Available: https://www.stretchsense.com/article-resources/case-study/capacitive-vs-resistive-strainstretch-measurement/. [Accessed: 21-May-2019].
[42] “CS15 Datasheet.” [Online]. Available: https://www.singletact.com/SingleTact_Datasheet.pdf. [Accessed: 21-May-2019].
[43] “Migamotors.” [Online]. Available: https://www.migamotors.com/Media/MAD-V5-TechNote.pdf. [Accessed: 21-May-2019].
[44] N. Akhter, S. Tharewal, H. Gite, and K. V. Kale, “Microcontroller based RR-Interval measurement using PPG signals for Heart Rate Variability based biometric application,” *2015 International Conference on Advances in Computing, Communications and Informatics (ICACCI)*. 2015.
[45] “Heartbeats in Your Project, Lickety-Split,” *World Famous Electronics llc.* [Online]. Available: https://pulsesensor.com/. [Accessed: 21-May-2019].
[46] “Heartbeats in Your Project, Lickety-Split,” *World Famous Electronics llc.* [Online]. Available: https://pulsesensor.com/. [Accessed: 21-May-2019].
[47] K. R. Knecht, J. D. Seller, and B. S. Alpert, “Korotkoff Sounds in Neonates, Infants, and Toddlers,” *The American Journal of Cardiology*, vol. 103, no. 8. pp. 1165–1167, 2009.
[48] K. Y. Chin and R. B. Panerai, “Relating external compressing pressure to mean arterial pressure in non-invasive blood pressure measurements,” *Journal of Medical Engineering & Technology*, vol. 39, no. 1. pp. 79–85, 2015.
[49] A. Chandrasekhar, C.-S. Kim, M. Naji, K. Natarajan, J.-O. Hahn, and R. Mukkamala, “Smartphone-based blood pressure monitoring via the oscillometric finger-pressing method,” *Science Translational Medicine*, vol. 10, no. 431, 2018.

# Annex A

## Instructions of Use

## SMART JACKET

### INSTRUCTIONS OF USE

**Standardized protocol for blood pressure measurement in premature infants [49].**

- Measure 1.5h after a feed or medical intervention.
- Select the appropriate sized bracelet (Small, Medium or Large).
- After the pressure bracelet placement, left the infant undisturbed for 15 min.
- Infant asleep or in quiet and controlled awake state.
- 3 successive BP readings at 3min intervals.

#### Initialization

1-Holding the smart jacket on your hands, press the Lilypad Simblee ON button for starting the connection.

2-Remark the initial lighting of the orange LED indicator, which ensures there's enough battery in the smart jacket. Oppositely, it is compulsory to connect the Lilypad Simblee board to the PC using an USB cable which will effectively charge it. Wait for 45 min, for full charge.

3-With your Android or iOS device Bluetooth on, open the "Simblee APP" (Install it from your app manager if you don't have it yet) and wait until the "X Blood Pressure" sign pops out, and then click on it. You must remain within the 10 meters range, otherwise a connection lost message will pop out.

#### Calibration

4-Once inside the APP, go to the Control tab and proceed to calibrate the jacket. To do so, just press on **Check Press** button and if the resulting value is approx. 0 mmHg the jacket is properly calibrated. Otherwise, contact to the technician in duty.

#### How to put on the jacket

5-Put on the jacket to the patient following the pattern: Left arm, right arm and close up chest buttons. The optical sensor must be **placed at the wrist**, under the jacket slope and fastened using the velcro strap. Make sure, the green light is aiming to the skin direction.

The pressure bracelet, is fastened firstly, to the jacket using the snap buttons. Then wrapped around the right upper arm, at an approx. distance of **one inch from the cubital fossa** or elbow pit, and eventually, fastened using the snap buttons.

6-Place the pressure sensor straight to the surface of the bracelet, in between the bracelet and the jacket. **The sensor's circumference must be fully covered under the bracelet.**

7-Pressing the "Check press" button, make sure that the value representing the initial pressure, is lesser than 22 mmHg. Oppositely, carefully adjust the bracelet or the position along the jacket.

## BP Measurement

8-**Never start a measurement if the temperature is higher than 30ºC.**

9-Slide the "ON Measure" button to initiate the blood pressure measurement. The algorithm, will firstly, make sure the initial pressure is lesser than 22 mmHg or pop out the message "ERROR of initial pressure". Secondly, the BPM will be calculated via two methods and compared for ensuring the reliability of the measurement. If succeed, the message **"Waiting for push button"** will pop out. Carefully, press the push button UNTIL the message "**Release push button"** is printed. Meanwhile, and only when the push button is actioned, the bracelet pressure will increase. If involved in the event of threatening situation, just release the push button and immediately, release the bracelet from the jacket. When succeed in compressing the bracelet, the "**Measuring PS**" message will pop out and eventually, the systolic, diastolic and mean pressure values printed and saved in the "Register" tab. Oppositely, if there was an error in the measurement it will be printed the message "**ERROR, try again**".

10- Once the blood pressure measurement is completed, release the bracelet from the jacket and place it far from the patient's reach. **Don't perform a new measurement for 3 min.**

# Annex B

## Second prototype CAD

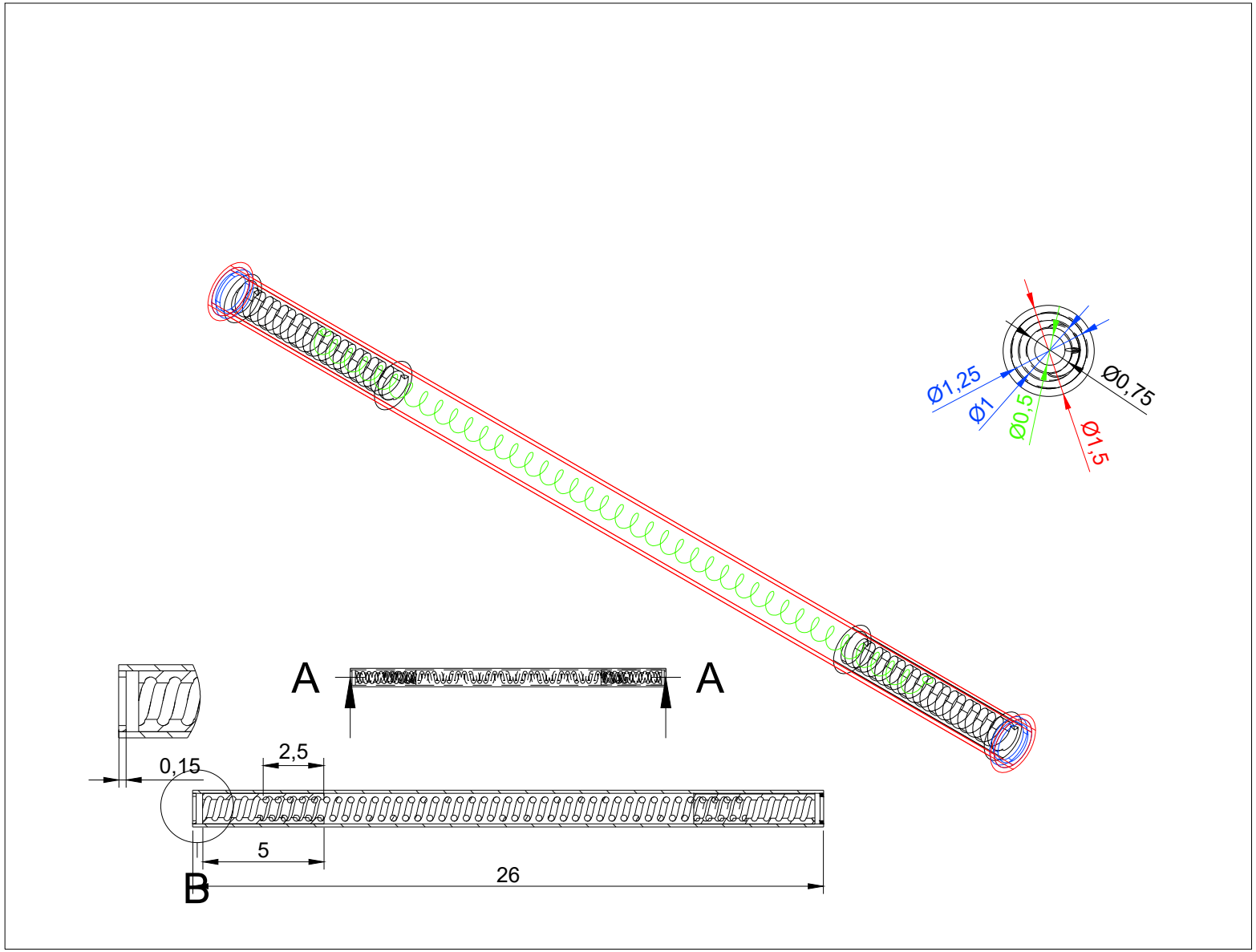

# Annex C

## Total energy consumption calculation

$$0.065kW(W\ ASUS\ laptop) \cdot \frac{3hour}{day} \cdot \frac{170days}{project} = 33.15kWh$$